



Science Arts & Métiers (SAM)

is an open access repository that collects the work of Arts et Métiers Institute of Technology researchers and makes it freely available over the web where possible.

This is an author-deposited version published in: <https://sam.ensam.eu>
Handle ID: <http://hdl.handle.net/10985/18699>

To cite this version :

Jacques VERDU, Xavier COLIN - Thermooxidative and thermohydrolytic aging of composite organic matrices - 2011

Any correspondence concerning this service should be sent to the repository

Administrator : scienceouverte@ensam.eu



THERMOOXIDATIVE AND THERMOHYDROLYTIC AGING OF COMPOSITE ORGANIC MATRICES

Xavier Colin and Jacques Verdu

ARTS ET METIERS ParisTech, PIMM, Paris, France

ABSTRACT

This chapter deals with the main causes of chemical ageing in organic matrix composites: hydrolysis, essentially in polyesters and polyamides, and oxidation in all kinds of polymer matrices. The first section is devoted to common aspects of chemical degradation of organic matrices. It is shown that chain scission and, at a lesser extent, crosslinking are especially important because they induce embrittlement at low conversions. Quantitative relationships between structural parameters and mechanical properties are briefly examined. The second section deals with diffusion–reaction coupling. In the cases of hydrolysis and oxidation, kinetics can be limited by respectively water and oxygen diffusion. Then, degradation is confined in a superficial layer, that can carry important consequences on use properties. The third section is devoted to hydrolysis. The kinetic equations are presented in both cases of non equilibrated and equilibrated hydrolysis. Structure–stability relationships are briefly examined. Osmotic cracking process, very important in the case of glass fiber/unsaturated polyester composites, is described. The last section is devoted to thermal oxidation. The simplest kinetic models are presented. The main gravimetric behaviours are explained. A mechanism is proposed for the “spontaneous cracking” in the superficial layer of oxidized samples.

Key words: Degradation; Embrittlement; Chain scission; Hydrolysis; Water sorption; Oxidation; Diffusion–reaction coupling.

INTRODUCTION

There are many domains, for instance aeronautics, automotive or electrical engineering, where organic matrix composites are used for long times at temperatures higher than the

ambient temperature, but lower than the matrix heat deflection temperature (HDT). This latter is close to the glass transition temperature T_g for amorphous polymers:

$$\text{HDT} \approx T_g - \Delta T \quad \text{where } \Delta T \approx 5\text{--}10 \text{ K}$$

It is intermediary between T_g and the melting point T_f for semi-crystalline polymers, typically:

$$\text{HDT} \approx T_f - \Delta' T \quad \text{where } \Delta' T \approx 40\text{--}100 \text{ K}$$

In this temperature range, common industrial fibers (glass, carbon, Kevlar, etc ...) are stable, so that composites perish always by matrix degradation. Organic matrices can undergo structural changes belonging to two categories and having eventually opposite effects on use properties. The first category corresponds to processes of which the cause is an initial thermal instability. Post-cure in thermosets, post-crystallization in semi-crystalline thermoplastics or structural relaxation (physical aging) in amorphous polymers belong to this category. Their main common characteristic is that their kinetics is atmosphere independent and only depends on thermodynamic variables (temperature and stress state). Another common characteristic of these processes is that the amplitude of their effects sharply depends on processing conditions, especially on their thermal history at the end of processing operations.

These processes, which are mainly ascribable to polymer synthesis chemistry (post-cure) or polymer physics (crystallisation, structural relaxation) will not be considered here. As a matter of fact, they can affect the polymer behaviour, especially in the early part of its lifetime, but they are generally not the main cause of its failure.

The second category of structural changes corresponds to the cases of chemical interaction between the polymer and environmental reagents, especially oxygen and water. These processes have two important common characteristics: first, they induce random chain scission, which is the cause of deep embrittlement at low conversions. Second, they are diffusion controlled, i.e. they affect only a more or less thick superficial layer and thus, induce thickness degradation gradients, a characteristic which cannot be ignored in a durability analysis.

This chapter will be divided into four main sections: The first one devoted to common aspects of chemical degradation processes, the second one devoted to reaction–diffusion coupling, the third one focused on hydrolysis processes and the fourth one on thermo-oxidative aging. Durability problems will be considered essentially from the point of view of materials science rather than chemical mechanisms. Emphasis will be put on consequences of aging on mechanical properties.

COMMON ASPECTS OF CHEMICAL DEGRADATION PROCESSES

Structural changes induced by chemical aging can be ranged into four categories depending on the affected structural scale (Table 1).

Table 1. The four scales of structure and the corresponding tools of investigation.

Structural scale	Entity	Main analytical tools	Theoretical tools
Molecular	Group of atoms Monomer unit	IR and NMR spectrometry	Organic chemistry
Macromolecular	Chain Network strand Crosslink	Viscosimetry SEC Sol-gel analysis	Macromolecular physico-chemistry
Morphological	Crystalline lamellae Spherulite	SAXS, WAXS, DSC SEM, TEM, AFM	Materials science
Macroscopic	Skin-core structure	Visible microscopy Modulus profiling Nano- and macro-indentation	Materials science

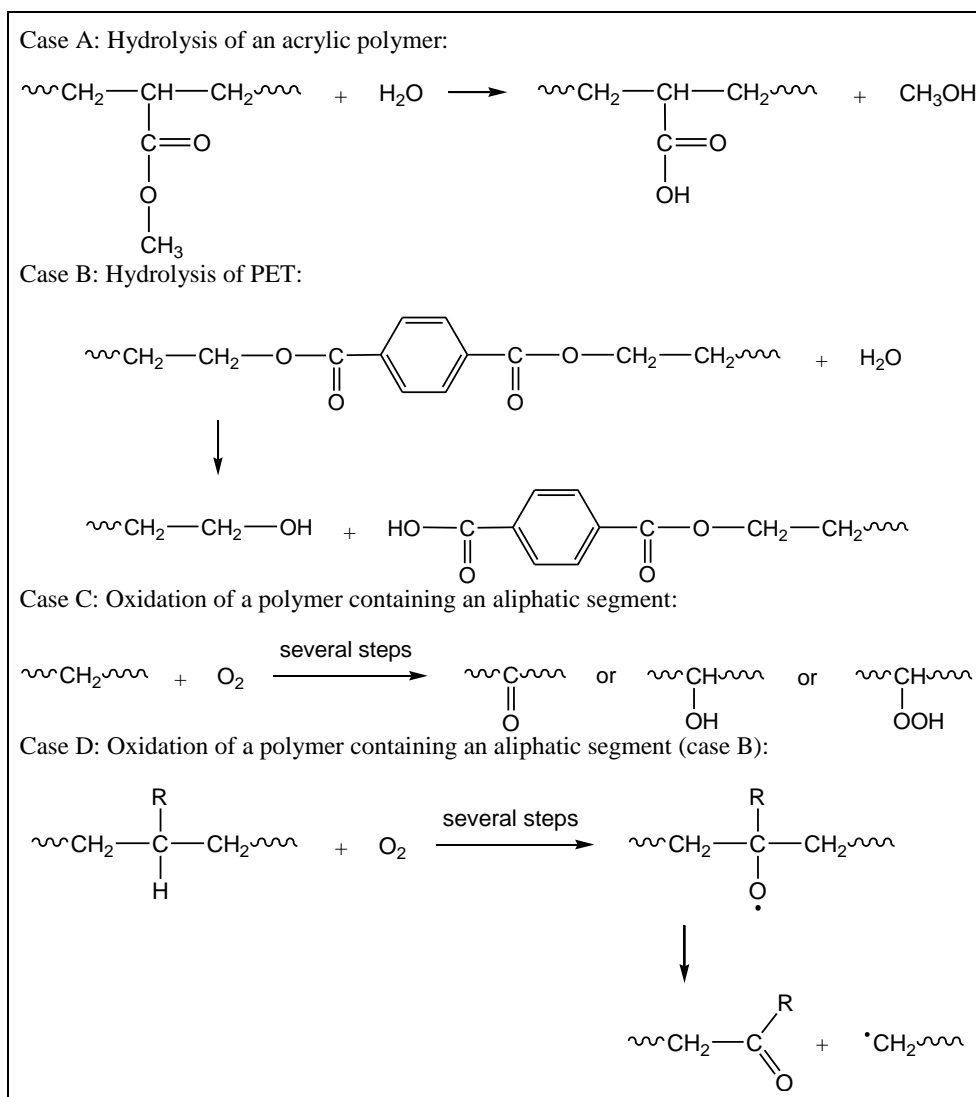


Figure 1. Examples of hydrolysis (A, B) or oxidation (C, D) processes leading (B, D) or not (A, C) to chain scission.

The “target” of water or oxygen attack is always the molecular scale, i.e. a region of sub-nanometric dimension. Some examples of chemical transformations at this scale are presented in Fig. 1. One can distinguish two categories of chemical events: those which do not affect the structure at the macromolecular scale and those (chain scissions, crosslinking) which affect the structure at the macromolecular scale. This distinction is based on a very simple rule: Only the structural changes at the macromolecular scale can have consequences on the polymer mechanical behavior at reasonably low conversions.

Hydrolysis without chain scission occurs only in acrylic and vinylic polymers with ester side groups. These polymers families are not very frequently used in composite matrices. Oxidation leads to predominating chain scission in the great majority of cases, to predominating crosslinking in some cases such as polybutadiene (Coquillat et al. 2007). An important quantity is the yield y of chain scission (y_s) or crosslinking (y_x) expressed as the number of broken chains or crosslinks formed per oxygen molecule absorbed. There is, to our knowledge, no case of industrial polymer for which this yield would be null.

1. Changes of Side-Groups

As previously seen, a change of side-groups, for instance the replacement of an ester by an acid (case A in Fig. 1), or the replacement of a methylene by a ketone or an alcohol (case C in Fig. 1), has no effect on mechanical properties. It can however affect other physical properties, for instance:

- Color if the new group is a chromophore: Hydrolysis has generally no consequences on color. In contrast, oxidation induces yellowing in practically all the aromatic polymers because it can transform some aromatic nuclei into quinonic structures absorbing in the violet–blue part of the visible spectrum and thus appearing yellow.
- Replacement of a non polar group by a polar group, for instance an ester by an acid (case A in Fig. 1) or a methylene by an alcohol (case C in Fig. 1) is expected to have the following consequences:
 - Increase in dielectric permittivity;
 - Increase in refractive index;
 - Growth of dielectric absorption bands;
 - Increase in hydrophilicity and wettability.

These changes are rarely decisive in the case of composites.

2. Chain Scission

2.1. Random Versus Selective Chain Scission

Chain scissions can occur on peculiar sites having an especially high reactivity. In this case, they will be named “selective chain scissions”. Chain scissions can be also randomly distributed (i.e. all the repeat units are equireactive). In this case, they will be named “random chain scissions”.

The different types of scissions are schematized in Figure 2.

For composite matrices, in the context of long term hydrolytic or oxidative ageing, random chain scission predominates over all the other processes in the great majority of cases. Depolymerization occurs essentially at high temperatures, only in polymers having weak monomer–monomer bonds (e.g. poly(methyl methacrylate) and poly(oxymethylene)). Crosslinking predominates mainly in unsaturated polymers, i.e. essentially polybutadiene and its copolymers (Coquillat et al. 2007). Some exceptions are known in the domain of composite matrices, they will be examined in a short paragraph.

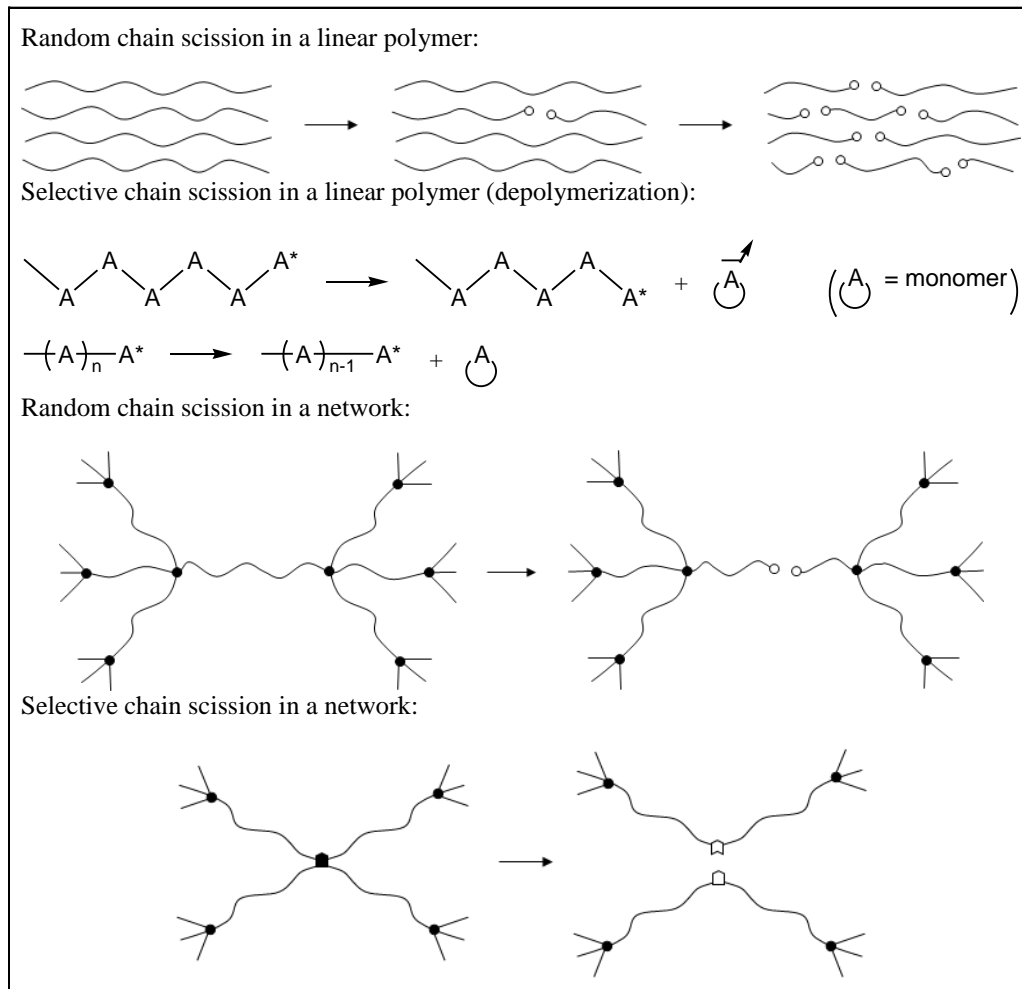


Figure 2. Random and selective chain scissions in linear and tridimensional polymers.

2.2. Random Chain Scission in Linear Polymers

The random character results from the fact that all the reactive groups of the macromolecules have an equal probability to react. This means that the probability for a chain to react is an increasing function of its length. The number (M_n) and weight (M_w) average molar masses are linked to the number S of chain scissions per mass unit by the following relationships (Saito 1958a and 1958b):

$$\frac{1}{M_n} - \frac{1}{M_{n0}} = S \quad (1)$$

$$\frac{1}{M_w} - \frac{1}{M_{w0}} = \frac{S}{2} \quad (2)$$

The polydispersity index IP varies as follows:

$$IP = IP_0 \frac{1 + S M_{n0}}{1 + \frac{IP_0}{2} S M_{n0}} \quad (3)$$

One sees that IP increases when $IP_0 < 2$, decreases when $IP_0 > 2$, but in all cases, tends towards 2 when the number of chain scissions increases. This characteristic is generally used to recognize a random chain scission.

Steric exclusion chromatography (SEC) can be used to determine the molar mass distribution (MMD) and the average values M_n and M_w . M_w can be also determined by viscosimetry using a power law:

$$\eta = K M_w^a \quad (4)$$

η is the intrinsic viscosity in the case of dilute polymer solution. In this case $a \approx 0.7$ and K depends on temperature and solvent nature.

η is the Newtonian viscosity in the case of molten polymer. In this case $a = 3.4$ and K depends on temperature and polymer chemical structure.

2.3. Consequences of Random Chain Scission on Thermodynamical Properties

2.3.1. Glass Transition Temperature T_g

According to Fox and Flory (1954):

$$T_g = T_{g\infty} - \frac{K_{FF}}{M_n} \quad (5)$$

where K_{FF} and $T_{g\infty}$ are increasing functions of the chain stiffness.

$$K_{FF} \propto T_{g\infty}^2 \text{ (Richaud et al. 2010)} \quad (6)$$

From Eqs (1) and (5), one obtains:

$$(T_{g0} - T_g) = K_{FF} S \quad (\text{Richaud et al. 2010}) \quad (7)$$

T_g decreases linearly with the number of chain scissions. The effect of these latter is an increasing function of the chain stiffness. Practically, T_g changes due to degradation of flexible polymers, having typically T_g values lower than 100°C , are negligible. In contrast, they can be measured in the stiff polymers, especially those having aromatic groups in the chain.

2.3.2. Melting Point

In semi-crystalline polymers, degradation is accompanied of morphological changes (see below) and it is not easy to separate the (small) effects of molecular mass decrease from those of morphological changes. To resume, degradation induces only small variations of the melting point and the sense of this variation can vary from a polymer to another. Melting point measurement is thus not an adequate method to monitor random chain scission.

2.3.3. Elastic Properties

At the conversions of practical interest, random chain scissions have no significant effect on elastic properties of linear polymers.

2.3.4. Fracture Properties

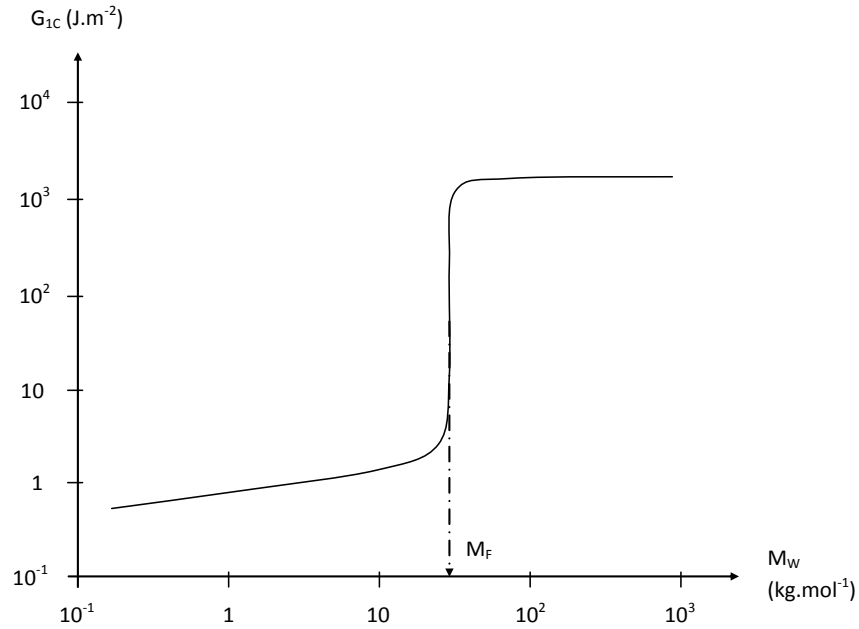


Figure 3. Shape of the variation of the crack propagation energy (critical rate of elastic energy release) with the weight average molar mass (for instance Greco and Ragosta 1987).

The effect of molar mass on toughness of linear polymers is schematized in Figure 3. For all the polymers, one can distinguish two regimes separated by a relatively sharp transition at a critical molar mass M_F . At molar masses lower than M_F , the polymers are extremely brittle,

their toughness is only due to Van der Waals interactions. At molar masses higher than M_F , the polymers have a toughness often in the 10^3 – 10^4 J.m⁻² range, almost independent of molar mass. In amorphous polymers, M_F is mainly linked to the entanglement density. As a matter of fact, plastic deformations responsible for the high toughness, are linked to chain drawing and this latter is possible only if the chains participate to a network, here the entanglement (topological) network.

In semi-crystalline polymers, the critical quantity is the interlamellar spacing l_a . For instance polyethylene (Kennedy et al. 1994) or polyoxymethylene (Fayolle et al. 2009) are brittle when $l_a \leq 6$ nm. Since l_a is sharply linked to molar mass, it can be considered, for these polymers also, that there is a critical molar mass M_F separating brittle and ductile domains (Fayolle et al. 2008).

It can be interesting to establish a relationship between M_F and the entanglement molar mass M_E , this latter being sharply linked to the chemical structure (Fetters et al. 1999). It appears that:

- For amorphous polymers (Kausch 2001) and semi-crystalline polymers of low crystallinity:

$$\frac{M_F}{M_E} \approx 2 \text{ to } 10 \quad (8)$$

- For relatively highly crystalline polymers (Fayolle et al. 2008):

$$\frac{M_F}{M_E} \approx 50 \quad (9)$$

According to the shape of Figure 3, the effect of random chain scission must display three characteristics:

- 1) If the initial molar mass is high enough, chain scission is expected to have no effect on fracture properties in the initial period of exposure, before molar mass reaches the critical value.
- 2) Toughness must decay abruptly of one to three decades when molar mass reaches the critical value.
- 3) Beyond the ductile–brittle transition, the toughness decreases continuously but very slowly. The change of toughness with the number of chain scissions S is expected to be the mirror image of Figure 3 (see Figure 4).

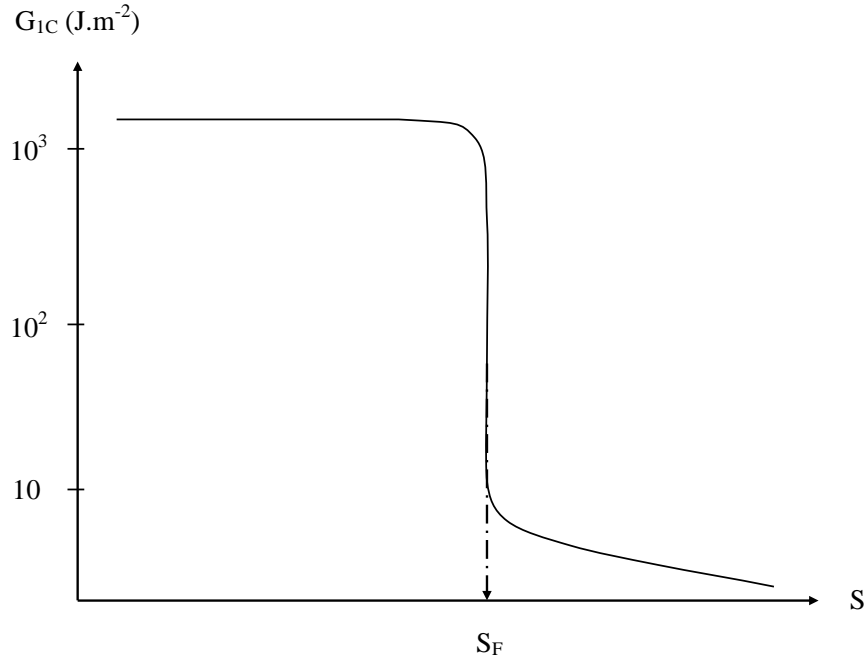


Figure 4. Expected shape of the variation of toughness with the number of chain scissions per mass unit.

The critical number of chain scission S_F for embrittlement is given by Equ. 2:

$$S_F = 2 \left(\frac{1}{M_F} - \frac{1}{M_{W0}} \right) \quad (10)$$

In any case: $M_F > 10 \text{ kg.mol}^{-1}$, so that:

$$S_F \leq \frac{2}{M_F} \approx 0.2 \text{ mol.kg}^{-1} \quad (11)$$

In common industrial thermoplastics, the monomer concentration $[m]$ is such as:

$$[m] > 2 \text{ mol.kg}^{-1} \quad (12)$$

It appears that embrittlement occurs always at a small conversion degree of the chain scission process. In certain cases, for instance polypropylene (Fayolle et al. 2002), embrittlement occurs while no structural change is observable by IR.

2.3. Random Chain Scission in Networks

Let us consider an ideal network in which every chain is connected to network nodes at both extremities. Such chains are called: “elastically active chains” (EAC). Their concentration v_0 is linked to the concentration x_0 of nodes by:

$$v_0 = \frac{f}{2} x_0 \quad (13)$$

where f is the node functionality, i.e. the number of chains connected to a node.

If the network undergoes S random chain scissions with $S \ll v_0$, each chain scission occurs in an EAC, so that new crosslink density is given by (Pascault et al. 2002):

$$v = v_0 - jS \quad (14)$$

with $j = 3$ for $f = 3$, and $j = 1$ for $f > 3$ (see Figure 5).

Each chain scission creates two dangling chains.

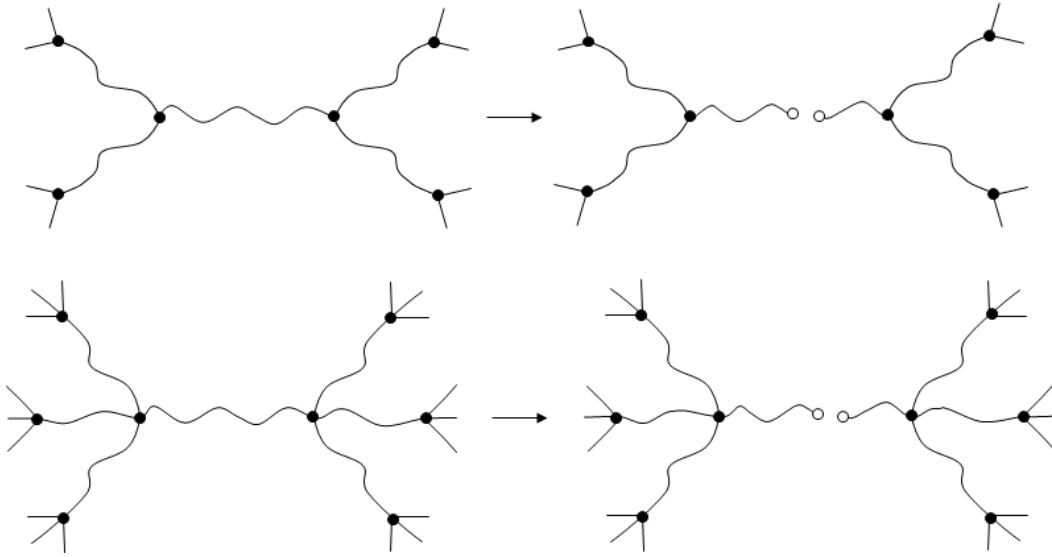


Figure 5. Schematization of a random chain scission in a network with trifunctional (above) and tetrafunctional (below) nodes.

Indeed, chain scission transforms an ideal network in a non-ideal one and the probability to have a chain scission in a dangling chain increases with the number of chain scissions (see Figure 6).

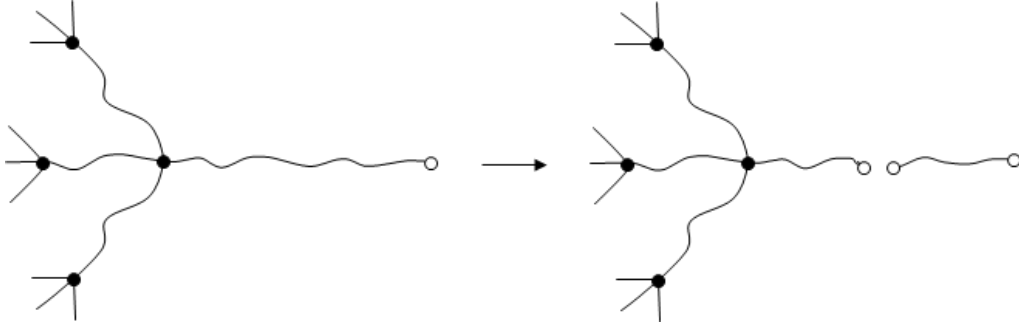


Figure 6. Schematization of a chain scission in a dangling chain.

At a given state of degradation, the mass fraction w_e of EAC is:

$$w_e = v M_e \quad (15)$$

Let us consider a chain scission process at a constant rate: $r = dS/dt$, for instance in a network having nodes of functionality $f > 3$. The probability to break an EAC is expected to be proportional to the EAC mass fraction so that:

$$\frac{dv}{dt} = -r w_e = -r M_e v \quad (16)$$

So that:

$$v = v_0 \exp -r M_e t \quad (17)$$

Although the chain scission process determined by the chemical mechanism is an apparent zero order process, the crosslink density is expected to decrease in an apparent first order process. In practice, however, the mechanical behavior is strongly altered at relatively low conversions, before the probability to have a scission in a dangling chain has reached a significant value. It is noteworthy that chain scissions on dangling chains create free chains. The amount of these latter corresponds to the extractable fraction in solvents.

Analytical methods for the determination of the number S of chain scissions per mass unit are scarce. When elastic properties in rubbery state are measurable, one can use the theory of rubber elasticity according which (Flory 1953):

$$\frac{dG}{dS} = \frac{dG}{dv} \frac{dv}{dS} = -j R T \rho \quad (18)$$

where G is the shear modulus at $T > T_g$ and ρ is the specific weight (kg.m^{-3}) of the polymer.

The glass transition temperature T_g is also dependent on crosslink density. According to Di Marzio (1964):

$$T_g = \frac{T_{gl}}{1 - K_{DM} F v} \quad (19)$$

where T_{gl} and F are parameters depending on the chain stiffness and K_{DM} is an universal constant ($K_{DM} \approx 2$).

$$\frac{dT_g}{dS} = -j \frac{T_g}{dv} = \frac{j K_{DM} F T_{gl}}{(1 - K_{DM} F v)^2} = j K_{DM} F \frac{T_g^2}{T_{gl}} \quad (20)$$

The effect of chain scissions is thus an increasing function of T_g .

Let us consider, for instance, an epoxy network based on the triglycidyl derivative of p-aminophenol (TGAP) crosslinked by diaminodiphenylmethane (DDM) in stoichiometric proportion. The characteristics (Pascault et al. 2002) are:

$$T_g = 494 \text{ K}, F = 23 \text{ g.mol}^{-1}, T_{gl} = 293 \text{ K}, j = 3 \text{ (trifunctional crosslinks)}.$$

Then:

$$\frac{dT_g}{dS} = 172 \text{ K.kg.mol}^{-1} \quad (21)$$

2.4. Consequences of Chain Scission on Mechanical Properties

The effect of chain scissions on elastic properties depends on the amplitude of the dissipation peak linked to the β relaxation. For polymers having a weak β transition, for instance styrene crosslinked polyesters or vinylesters, chain scissions have practically no effect on elastic properties in glassy state.

For polymers having a strong β transition, for instance diamine crosslinked epoxies, chain scissions lead to a modulus increase in the modulus plateau between the β transition and the glass transition (Figure 7). The phenomenon has been called “internal antiplasticization” (Rasoldier et al. 2008). It can be evidenced through nano- or micro-indentation profiles to characterize degradation gradients in the sample thickness (Olivier et al. 2009).

Chain scissions induce a decrease of fracture toughness. From this point of view, degraded networks differ from ideal networks in which fracture properties are generally a decreasing function of crosslink density (Crawford and Lesser 1999, Pascault et al. 2002). Little is known on the quantitative relationships between chain scission and embrittlement in networks.

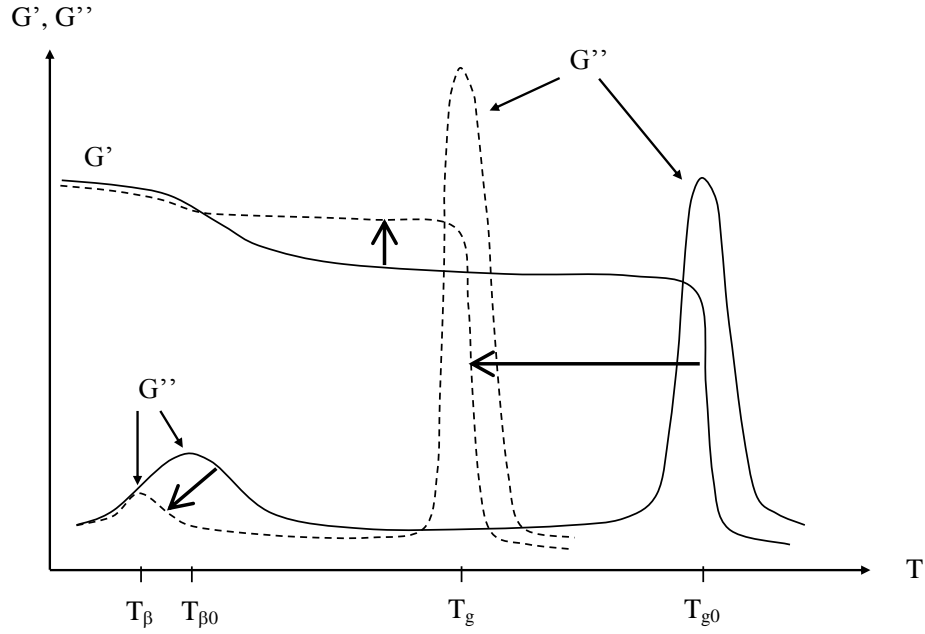


Figure 7. Storage (G') and dissipation (G'') modulus against temperature for a network having a strong β transition before (full line) and after (dashed line) chain scission.

3. Simultaneous Chain Scission and Crosslinking

3.1. In Linear Polymers

Saito's equations become:

$$\frac{1}{M_n} - \frac{1}{M_{n0}} = S - X \quad (22)$$

$$\frac{1}{M_w} - \frac{1}{M_{w0}} = \frac{S}{2} - 2X \quad (23)$$

where X is the number of crosslinks and S the number of chain scissions.

There is an "equilibrium" corresponding to the constancy of M_w , i.e. to:

$$S = 4X \quad (24)$$

For $X > S/4$, crosslinking predominates over chain scissions. Polymer gelation occurs when $M_w \rightarrow 0$, i.e. when:

$$\frac{S}{2} - 2X = -\frac{1}{M_{w0}} \quad (25)$$

i.e. in the absence of chain scission for:

$$X_g = -\frac{1}{2M_{w0}} \quad (26)$$

Beyond the gel point, an insoluble fraction appears. According to Charlesby and Pinner (1959), the soluble fraction w_s is linked to the number of chain scissions and crosslinks by:

$$w_s + w_s^{1/2} = \frac{S}{2X} + \frac{1}{M_{w0} X} \quad (27)$$

3.2. Consequences of Crosslinking on Properties

In linear polymers, crosslinking affects mainly rheological properties in molten state. As a matter of fact, long branching is responsible for the disappearance of the Newtonian plateau (Figure 8).

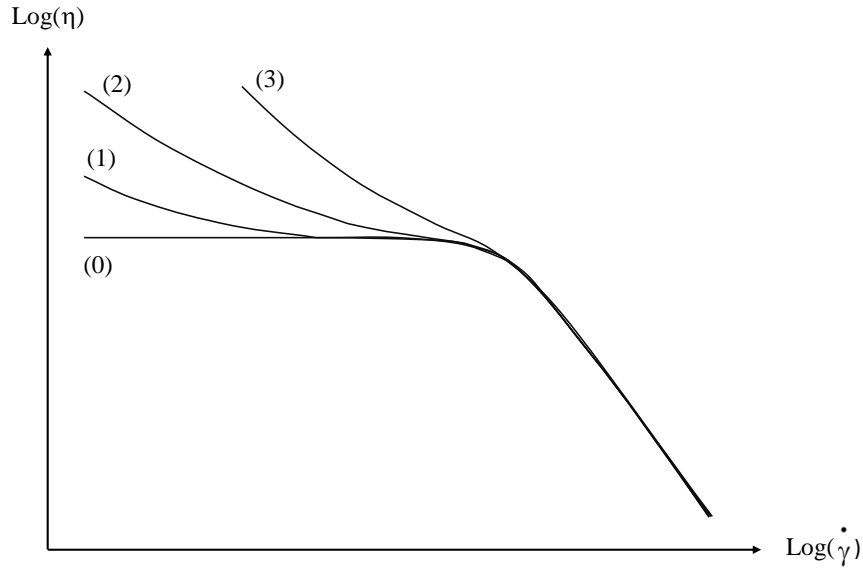


Figure 8. Shape of the curve Log(viscosity) versus Log(shear rate) for a linear polymer before (0) and after ageing leading to an increase of the degree of branching ($0 < 1 < 2 < 3$).

Crosslinking induces an increase in the glass transition temperature. In the case of simultaneous chain scission and crosslinking, it can be written, in a first approach:

$$T_g = T_{g0} + k_S S + k_X X \quad (28)$$

k_S is significantly higher than k_X . As an example, in bisphenol A polysulphone, $k_S/k_X \approx 2.1$ (Richaud et al. 2010). In other words, crosslinks have less influence than chain scission on T_g .

The effects of crosslinking on fracture properties are not well known. In most cases, crosslinking is expected to induce embrittlement according to the following causal chains:

- 1) Crosslinking \rightarrow Increase in T_g \rightarrow Increase in yield stress \rightarrow Ductile (plastic) deformation less and less competitive with brittle deformation
- 2) Crosslinking \rightarrow Shortening of EAC \rightarrow Decrease in drawability of EAC \rightarrow Reduction of the plastic zone at crack tip \rightarrow Decrease in toughness

3.3. Post-Cure

In most cases of industrial thermosets, cure is not complete, reactive groups remain trapped in glassy state at the end of processing operations. In ageing conditions, they can recover mobility enough to react, because they are heated at temperatures not very far from T_g or the polymer is plasticized by water. Then, cure reactions are reactivated, the crosslink density increases in an autoretardated way and stops when all the available reactive groups have been consumed. Except for scarce cases, for instance epoxides crosslinked by unsaturated anhydrides (Le Huy et al. 1993), oxidative ageing is dominated by chain scission, so that, for thermosets, crosslink density variations during thermal ageing have the shape of Figure 9.

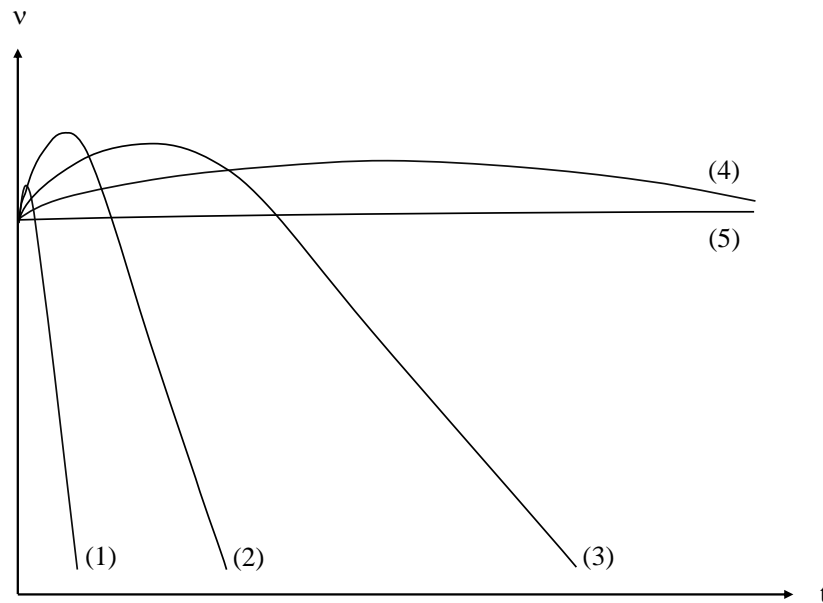


Figure 9. Shape of kinetic curves of crosslink density variations during the thermal ageing (in air) of a thermoset at various temperatures: $T_1 > T_2 > T_3 > T_4 > T_5$.

These curves can be decomposed into two components, i.e. post-cure and degradation (see Figure 10).

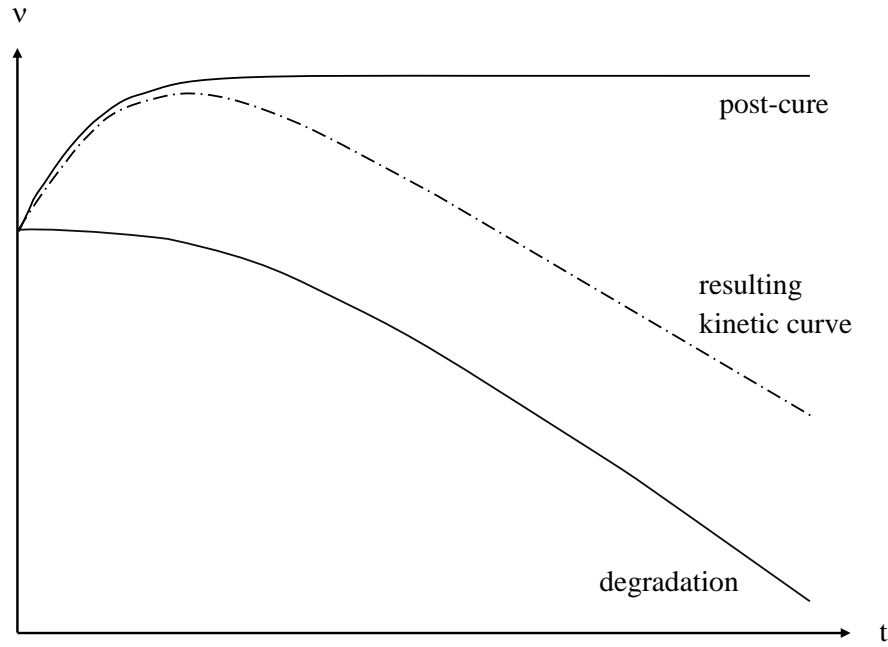


Figure 10. Schematization of combined effects of post-cure and degradation.

In the simplest cases, there is no interaction between both processes, so that their effects on crosslink density are additive. In other cases, however, oxygen or water can inhibit post-cure and a more complex behaviour can be expected.

REACTION–DIFFUSION COUPLING

In both cases of oxidation and hydrolysis, the polymer matrix reacts with a small molecule M (oxygen or water) coming from the environment. In a thin elementary layer at a distance z of the sample surface, the reactant concentration balance can be ascribed:

Reactant concentration change = Rate of reactant supply by diffusion – Rate of reactant consumption by reaction

The balance equation can be thus written, in the case of unidirectional diffusion, i.e. far from the sample edges:

$$\left(\frac{\partial C}{\partial t} \right)_z = D \frac{\partial^2 C}{\partial z^2} - r(C) \quad (29)$$

where C is the reactant concentration, D is the coefficient of reactant diffusion in the polymer and $r(C)$ is the rate of reactant consumption expressed as a function of the reactant concentration.

The resolution of Equ. 29 needs the knowledge of two physical quantities: the equilibrium concentration C_s of reactant and its coefficient of diffusion D in the polymer, and one chemical data: the concentration dependence $r(C)$ of the reactant chemical consumption.

1. Reactant Transport Properties

Concerning first transport properties in matrices and their relationships with polymer structure, there are various book chapters and monographs (Crank and Park 1968, Hopfenberg 1974, Van Krevelen 1976, Bicerano 2002). The main differences between oxygen and water properties can be summarized as follows: The oxygen solubility in polymers is always low, typically $\leq 10^{-3} \text{ mol.l}^{-1}$, practically insensitive to small structural changes. The coefficient of oxygen diffusion is of the order of $10^{-11} \pm 2 \text{ m}^2.\text{s}^{-1}$ at ambient temperature and its apparent activation energy in the $[30\text{--}60 \text{ kJ.mol}^{-1}]$ interval. Oxygen transport properties are practically always determined from permeability measurements. It can be reasonably assumed that, during an ageing experiment at constant temperature, D is independent of C and of reaction conversion at reasonably low conversions, for instance before and just after embrittlement.

Some relationships between the polymer structure and water transport characteristics are illustrated by Table 2.

Table 2. Molar mass of the constitutive repeat unit, water mass fraction at equilibrium at 50°C and 50% RH, coefficient of diffusion in the same conditions, and number of moles of water per constitutive repeat unit. Compiled data from Bellenger et al. (1994), Tcharkhtchi et al. (2000) and Gaudichet et al. (2008).

Polymer	code	M (g.mol ⁻¹)	m _{equ} (%)	D × 10 ¹² (m ² .s ⁻¹)	n (mol.mol ⁻¹)
Poly(methyl methacrylate)	PMMA	100	1.28	0.36	0.071
Poly(ethylene terephthalate)	PET	192	0.55	0.54	0.059
Polycarbonate	PC	254	0.25	5.4	0.035
Polyamide 11	PA11	183	1.5	0.13	0.153
Poly(bisphenol A) sulphone	PSU	442	0.52	8.97	0.128
Polyethersulphone	PES	232	1.8	2.79	0.232
Polyetherimide	PEI	592	1.4	0.97	0.460
Polypyromellitimide	PPI	382	5.0	0.1	1.061
Polyimide	IP960	486	4.2	0.83	1.134
Epoxy	DGEBA–Etha	858	2.0	1.03	0.953
Epoxy	DGEBD–Etha	578	6.8	0.11	2.183
Unsaturated polyester	UP	334	0.83	0.88	0.154
Vinylester	VE(D)	980	1.7	0.6	0.926
Vinylester	VE(C)	550	0.5	0.5	0.153

The main trends of structure–property relationships can be briefly summarized as follows:

a) Three main types of groups can be distinguished:

G1: Hydrocarbon and halogenated groups of which the contribution to hydrophilicity is negligible. Polymers containing only these groups (polyethylene, polypropylene, polystyrene, elastomers, etc ...) absorb less than 0.5 wt% water.

G2: Groups of relatively low polarity (ethers, ketones, esters, etc ...). Polymers containing only these groups (with hydrocarbon ones) absorb generally less than 2 wt% water. Physical effects of water absorption (plasticization, swelling) are generally negligible. Polymers containing the ester group (polyalkylene terephthalates, unsaturated polyesters, anhydride crosslinked epoxies, etc ...) are however susceptible to hydrolysis (see below). Polymers containing methacrylic esters (polymethyl methacrylate, vinyl esters) are generally resistant to hydrolysis.

G3: Highly polar groups able to establish strong hydrogen bonds with water (sulphones, alcohols, amides, acids, etc ...). These polymers can absorb up to 5 wt% water, that can induce considerable physical changes, for instance T_g decreases of about 10 K per percent water absorbed, swelling and damage by swelling stresses occur during the sorption or desorption transients.

- b) In each polymer family containing one type of hydrophilic group, for instance polyamides, polysulphones, polyimides, amine crosslinked epoxies, etc... the equilibrium water concentration increases non linearly with the concentration of polar groups. A theory based on the hypothesis that water is doubly bonded has been proposed to explain this behavior (Tcharkhtchi et al. 2000, Gaudichet-Maurin et al. 2008).
- c) The relationships between diffusion coefficient and polymer structure are not fully understood, but what is clear is that in a given family, D is a decreasing function of the water equilibrium concentration (Thominette et al. 2006). This dependence indicates that water-polymer hydrogen bonds slow down diffusion as well in polyethylenes (McCall et al. 1984) as in epoxies (Tcharkhtchi et al. 2000).
- d) Diffusion is thermally activated, apparent activation energies are generally in the 20–60 kJ.mol⁻¹ interval. Equilibrium water concentrations depend only slightly on temperature, that can be explained by considerations of heat of solubility (Merdas et al. 2002).

2. Chemical Reactant Consumption

2.1. Hydrolysis

Let's consider now the term representing the chemical reactant consumption in the reaction-diffusion equation (Equ. 29). In the simplest case of hydrolysis, $r(C)$ appears as a simple first order equation:

$$\frac{\partial C}{\partial t} = D \frac{\partial^2 C}{\partial z^2} - k[A]_0 C \quad (30)$$

where k is the second order rate constant of the water-polymer reaction, $[A]_0$ is the concentration of hydrolysable groups, considered constant at reasonably low conversions.

A more complex equation is needed in the case where hydrolysis is equilibrated (see below). When Equ. 30 is an acceptable approximation, the integration for a symmetric sheet of thickness L gives:

$$C = C_s \frac{\cosh J \left(z - \frac{L}{2} \right)}{\cosh \frac{JL}{2}} \quad (31)$$

where $J = \frac{k[A]_0}{D}$

where the origin of z is taken at a sample edge.

The water concentration and thus, also, the hydrolysis rate, decreases in a pseudo-exponential way from the edges, where $C = C_s$, to the middle of the sample where $C = C_m$ (minimum).

When $C = 6 J^{-1}$, $C_m / C_s \approx 0.1$. Thus, for $L \gg 6 J^{-1}$, the sample behaves as a sandwich made of an undegraded core with two degraded superficial layers.

In the case of equilibrated hydrolysis, for instance for PA11 (Jacques et al. 2002), a degradation gradient appears at the beginning of exposure, but the sample tends to homogenize as the hydrolysis rate slows down.

2.2. Oxidation

The case of oxidation is more complex because the mechanism is a branched radical chain of which the kinetic modeling was considered out of reach for a long time. The first attempts were made at the beginning of 80's by Seguchi et al. (1981 and 1982) and Cunliffe and Davis (1982) in the simplest case of constant initiation rate, steady-state for radical concentration, long kinetic chain and low conversion. All these simplifying assumptions are more or less valid in some cases of radiochemical oxidation, but they are questionable in the case of thermal oxidation.

Assuming their validity, the rate of oxygen consumption can be expressed by an hyperbolic function of oxygen concentration:

$$r(C) = \frac{aC}{1 + bC} \quad (32)$$

where a and b can be expressed in terms of rate constants of the elementary reactions participating to oxidation.

The reaction-diffusion equation becomes then:

$$\frac{\partial C}{\partial t} = D \frac{\partial^2 C}{\partial z^2} - \frac{aC}{1 + bC} \quad (33)$$

There is no analytical solution for this equation, but approximations can be obtained for extreme cases, for instance:

$$C \gg b^{-1} \Rightarrow r(C) = \frac{a}{b} = r_s \quad (34)$$

$$\text{And } C \ll b^{-1} \Rightarrow r(C) = a C \quad (35)$$

In the second case, the same solution as for hydrolysis (Equ. 30) will be obtained. In the first case, however, the integration leads to a parabolic shape of the oxygen concentration profile:

$$C = C_s + \frac{r_s}{2D} (z - L)z \quad (36)$$

The concentration in the middle of the sample is:

$$C = C_s - \frac{r_s L^2}{8D} \quad (37)$$

3. Case of Composites

In the case of composites, new problems linked to the anisotropy of diffusion paths, the eventual role of interfacial diffusion and the role of preexisting or swelling induced damage appeared in the middle of 70's. The interest was mainly focused on the effect of humidity on carbon fiber/amine crosslinked epoxy composites of aeronautical interest. For the pioneers of this research (Shen and Springer 1976), the determination of diffusion kinetic laws appeared as the key objective. Various studies revealed that, in certain cases, diffusion in composites cannot be modeled by a simple Fick's law and that Langmuir's equation is more appropriate. Carter and Kibler (1978) proposed a method for the parameter identification. At the end of 70's, the kinetic analysis of water diffusion into composites became a worldwide research objective. A great quantity of experimental data was obtained. The results can be summarized as follows:

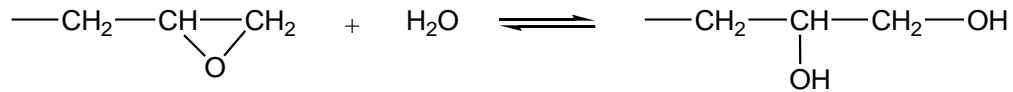
- a) Concerning the effect of fiber anisotropy on diffusion, a model for unidirectional composites was proposed by Kondo and Taki (1982). This model makes full account of the fact that water diffusivity is more privileged in the fiber direction than in the transverse one:

$$D_{//} = \frac{1 - V_f}{1 - 2\sqrt{V_f}/\pi} D_{\perp} \quad (38)$$

where $D_{//}$ and D_{\perp} are the respective diffusion coefficients in the longitudinal and transverse fiber directions.

Colin et al. (2005) showed that such models can also be used to predict oxygen diffusivity in composites. More recently, Roy and Singh (2010) showed that these models can be improved to take into account physical discontinuities such as highly permeable fiber/matrix interface or fiber/matrix debonding due to oxidative shrinkage and erosion.

- b) Concerning Langmuir's mechanisms, it was assumed, for a long time, that water was trapped in "defects" resulting from damage or preexisting, eventually located at interface. Tcharkhtchi et al. (2000) found that unreacted epoxide groups undergo a reversible hydrolysis:



Epoxide groups appear thus as "water traps" and are responsible for a Langmuir component in diffusion kinetic curves. Since industrial composites are rarely fully cured, it can be assumed that epoxide hydrolysis was often the cause of Langmuir's behavior in previous studies.

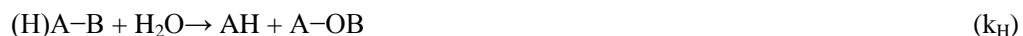
Recently, however, Derrien and Gilormini (2006) have found that Langmuir's behavior could be simply linked to the stress state induced by water diffusion.

- c) Concerning eventual interfacial processes, they raised up an abundant literature. Various techniques were used to characterize interfaces and interphases (Shradder and Block 1971, Di Benedetto and Scola 1980, Ishida and Koenig 1980, Rosen and Goddard 1980, Ishida 1984, Di Benedetto and Lex 1989, Thomason 1990, Hoh et al. 1990, Schutle and Mc Donough 1994). Round Robin tests showed that no one analytical method is able to give unquestionable results (Pitkethly et al. 1993). Even in the cases where the interface response to humid aging has been unambiguously identified from studies of model systems (Kaelble et al. 1975 and 1976, Salmon et al. 1997), it seems difficult, at this state of our knowledge, to build a non-empirical kinetic model of water effects on interface/interphase in composites.

HYDROLYSIS

1. Uncatalysed Hydrolysis Mechanisms and Kinetics in Pure Water

Hydrolysis is an ionic, step by step mechanism. In a first approach, the mechanism can be written:



The hydrolysis rate is thus:

$$\frac{d[A-B]}{dt} = k_R [AH][B-OH] - k_H [A-B][H_2O] \quad (39)$$

If S is the number of broken links, it can be written:

$$\frac{dS}{dt} = -\frac{d[A-B]}{dt} = -k_R (a_0 + S)(b_0 + S) + k_H w (e_0 - S) \quad (40)$$

where $a_0 = [AH]_0$, $b_0 = [B-OH]_0$, $e_0 = [A-B]_0$ and $w = [H_2O]$.

In the simplest cases, at reasonably low conversions, w is constant (no diffusion control) and $a_0 = b_0$, so that:

$$\frac{dS}{dt} = -k_R (a_0 + S)^2 + k_H w (e_0 - S) \quad (41)$$

The equilibrium corresponds to $S = S_e$ such as:

$$k_R (a_0 + S_e)^2 - k_H w (e_0 - S_e) = 0 \quad (42)$$

Two cases can be distinguished:

Case A: Hydrolysis reaches high conversions (case of most polyesters).

In this case, the reversible reaction can be neglected in a first approach and:

$$\frac{dS}{dt} = k_H w (e_0 - S) \quad (43)$$

$$\text{And } S = e_0 (1 - \exp - k_H w t) \quad (44)$$

At low conversions ($S \ll e_0$):

$$S \approx e_0 k_H w t = r_H t \quad (45)$$

Hydrolysis behaves as a pseudo zero order process with a quasi-constant rate r_H .

Case B: Equilibrium occurs at a low conversion (case of polyamide 11 (Meyer et al. 2002, Jacques et al. 2002)). Then, since ($S \ll e_0$), Equ. 41 can be simplified as:

$$\frac{dS}{dt} = -k_R (a_0 + S)^2 + k_H w e_0 \quad (46)$$

It is noteworthy that, in a linear polymer with no other chain end than AH and B-OH:

$$a_0 = \frac{1}{M_{n0}}, a_0 + S = \frac{1}{M_n} \text{ and } a_0 + S_e = \frac{1}{M_{ne}}$$

where M_{n0} , M_n and M_{ne} are the respective values of the number average molar mass at the beginning of exposure, after a time t of exposure and at equilibrium.

Resolution of the differential equation (46) leads to:

$$M_n = M_{n0} \frac{M_{n0}^{-1} + M_{ne}^{-1} + (M_{ne}^{-1} - M_{n0}^{-1}) \exp - K t}{M_{n0}^{-1} + M_{ne}^{-1} - (M_{ne}^{-1} - M_{n0}^{-1}) \exp - K t} \quad (47)$$

$$\text{where } M_{ne} = \left(\frac{k_R}{k_H e_0 w} \right)^{1/2} \quad (48)$$

$$\text{and } K = 2(k_R k_H e_0 w)^{1/2} \quad (48)$$

If the temperature dependence of water solubility can be represented by an Arrhenius law:

$$w = w_0 \exp - \frac{E_w}{RT} \quad (49)$$

and the activation energies of k_R and k_H are respectively E_R and E_H , one sees that the apparent activation energy of the equilibrium molar mass is:

$$E_{Mne} = \frac{1}{2}(E_R - E_H - E_w) \quad (50)$$

The apparent activation energy of the composite rate constant K is:

$$E_K = \frac{1}{2}(E_R + E_H + E_w) \quad (51)$$

Generally, $E_R \approx E_H \gg E_w$, so that $E_{Mne} \ll E_K$. The equilibrium value of molar mass is considerably less affected by temperature variations than the degradation rate at the onset of exposure. As an example, in PA11:

$$E_K = 97 \text{ kJ.mol}^{-1} \text{ and } E_{Mne} = -6.5 \text{ kJ.mol}^{-1} \text{ (Jacques et al. 2002).}$$

In thermosets, hydrolysis processes have been studied essentially in unsaturated polyesters crosslinked by styrene (UP). The problem raised up an abundant literature owing to the great technological importance of glass fiber-UP composites in boats, tanks, pipes, swimming pools, etc ... Before the beginning of 90's, however, kinetic modeling was

considered out of reach. Mortaigne et al. (1992) used rubbery modulus to determine the crosslink density according to Equ. 18. They used networks differing by the length of polyester prepolymers, i.e. by the concentration of dangling chains, to calibrate the measurements. Comparative studies (Bellenger et al. 1995, Belan et al. 1997) allowed to establish the following hierarchy of hydrolysis rate constants:

Unreacted fumarate > Reacted fumarate > Orthophthalate > Isophthalate >> Methacrylate(52)

The diol structure (and, indeed, the styrene concentration) affects mainly the hydrophilicity but does not influence significantly the hydrolysis rate constant, except for ethylene glycol which is more reactive than other diols. Vinylesters are, at least, one order of magnitude less reactive than UP.

A comparison of apparent zero order rate constants: $r_H = k_H e_0 w$, for linear and tridimensional polymers is given in Table 3.

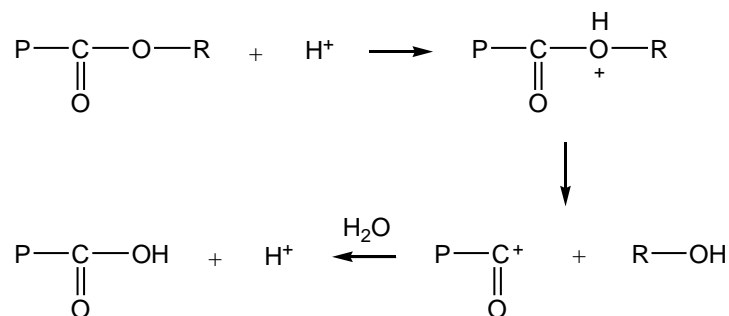
Table 3. Comparison of apparent zero order rate constants at 100°C and apparent activation energy for two linear (PC and PET) and two tridimensional polymer families (UP and VE) of ester containing polymers.

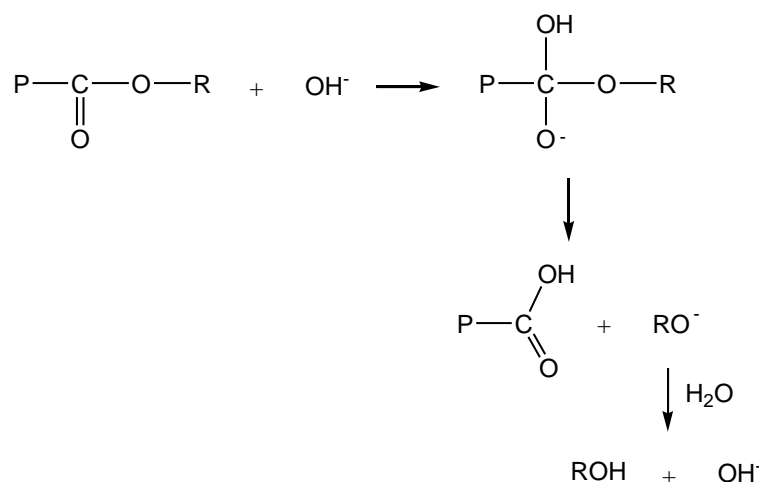
Polymer	Code	r_H at 100°C (mol.l ⁻¹ .s ⁻¹)	E_{act} (kJ.mol ⁻¹)	Reference
Polycarbonate	PC	6.7×10^{-9}	75	Pryde et al. 1982
Poly(ethylene terephthalate)	PET	6.0×10^{-8}	107	McMahon et al. 1959
Unsaturated polyester	UP	$(2 \text{ to } 15) \times 10^{-7}$	70 ± 10	Mortaigne et al. 1992
Vinylester	VE	$(2 \text{ to } 10) \times 10^{-9}$	—	Ganem et al. 1994

These comparisons show clearly that there is no influence of polymer architecture (tridimensional versus linear polymers) on hydrolysis kinetics. The observed differences are mainly due to differences in ester reactivity. Indeed, global hydrolysis rates depend also on water concentration, i.e. of water activity. In a first approach, one can consider that hydrolysis rate is proportional to the relative hygrometry.

2. Catalysed Hydrolysis Mechanisms and Kinetics

Hydrolysis can be catalyzed as well by H^+ as by OH^- ions. As an example, in polyesters:





Indeed, the first source of H^+ ions can be the acidic chain ends which accumulate into the polymer matrix during hydrolysis and which are expected to induce an autoacceleration of process. In fact these acids are weak and their dissociation is relatively disfavored in polymer matrices of low polarity. In PA11, they have no autocatalytic effect (Jacques et al. 2002). In PET, there is a relatively low autoacceleration which could be due only to the increase of polymer hydrophilicity linked to the accumulation of acid and alcohol groups resulting from hydrolysis (Ballara et al. 1989). The existence of an eventual autocatalysis in UP's is not obvious because it can be masked by osmotic cracking (see below). In contrast, an autocatalytic behavior has been recently observed in aliphatic polyesters of the polyadipate type (Coquillat et al. 2010).

Catalytic effects of H^+ or OH^- ions are, in contrast, clearly observed when the materials are immersed in acidic or basic solutions. It is noteworthy that ions are practically insoluble in nonpolar polymer matrices, so that two types of behavior can be observed:

- In the case of bases, there is only a superficial attack similar to erosion.
- In the case of acids, only undissociated species are soluble in the polymer, so that organic acids can be more active than mineral ones because they are more soluble. Concerning strong acids such as HCl, it has been observed that their effect increases almost exponentially when the pH of the solution decreases (Serpe et al. 1997), that can be explained by the fact that the undissociated form of the acid exists only at low pH value (Ravens 1960, Merdas et al. 2003).

3. Osmotic Cracking

Blistering of boat hulls made of glass fiber/polyester laminates led to worldwide catastrophic consequences on boat industry in the 80's. Blisters result from crack growth under the gel coat, parallel to the free surface. They were first observed by Ashbee and Wyatt (1969). Several interpretations were proposed in the following years, but it was finally recognized that the crack propagation results from an osmotic process (Fedors 1980). The mechanism can be briefly described as follows: If a crack is formed in a subcutaneous region,

it is rapidly filled by water coming from the bath. Water dissolves small organic (and eventually inorganic) molecules present in the polymer matrix. Then, the polymer layer separating the crack from the bath acts as a semi-permeable membrane, permeable to water but considerably less permeable to the solutes. Then, an osmotic pressure grows in the crack. According to Van't Hoff (1888):

$$\Delta p = RT \sum_{i=1}^n C_i \quad (53)$$

where C_i is the concentration of the i^{th} solute in water.

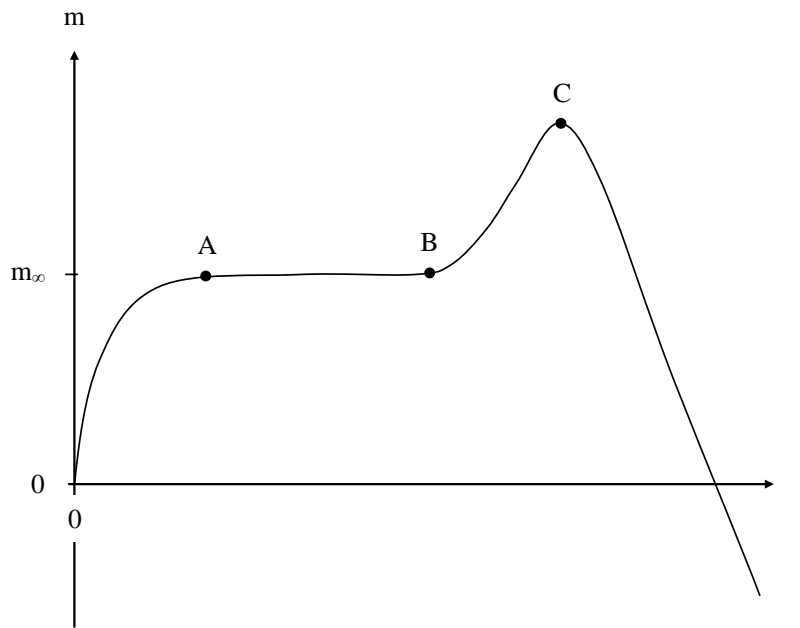


Figure 11. Shape of gravimetric curves in the case of osmotic cracking of thin samples. In A, the sorption equilibrium is reached. In B, cracking begins and increases the capacity of water absorption. In C, the cracks coalesce and the soluble organic molecules are lost in the bath.

Above a certain critical value depending on the polymer toughness, this pressure induces crack propagation (Walter and Ashbee 1982, Sargent and Ashbee 1984). Osmotic cracking can be put in evidence by gravimetry on relatively thin samples (Mortaigne et al. 1992) (Figure 11).

In the 80–90's, there were several studies aimed to establish the influence of initial composition (for instance, Abeysinghe et al. 1983) and the polymer structure (for instance, Mortaigne et al. 1992), on the osmotic cracking phenomenon. It was shown that it is faster and faster as:

- The initial concentration of organic molecules (unreacted monomers, initiator fragments, etc ...) increases.

-
- The initial concentration of dangling chains increases, i.e. the prepolymers molar mass decreases.
 - The hydrolysis rate increases.

Various explanations were proposed for the crack initiation mechanism. The only one consistent with all the available experimental data was proposed by Gautier et al. (1999) and can be briefly summarized as follows: Hydrolysis on dangling chains (initially present or resulting from hydrolysis events) generates small organic molecules. These latter (acid and alcohol terminated) are more polar than the polymer, so that their solubility in the matrix is limited. When they reach a critical concentration, they demix to form highly polar microdomains. Since these latter are more hydrophilic than the polymer, they absorb water and the osmotic cracking process begins. It is noteworthy that this process occurs because organic molecules have a smaller diffusivity than water, so that they accumulate in the timescale of hydrolysis. The resistance to osmotic cracking can be reduced by:

- Limiting the initial concentration of small molecules (initiators, catalysts, etc ...).
- Reducing the concentration of dangling chains, but the initial prepolymers length must be limited to facilitate processing.
- Reducing hydrolysis rate by: First, a decrease of polymer hydrophilicity by using nonpolar diols such as, for instance, neopentylglycol, and by increasing, when it is possible, the styrene content; Second, a decrease of ester reactivity by an appropriate choice of diacids (isophthalate rather than orthophthalate, etc ...).

Unfortunately, the “weakest point” of the polymer structure is the fumarate ester of which the replacement is difficult to envisage.

THERMAL OXIDATION

1. Introduction: General Aspects of Thermal Oxidation Processes

Thermal oxidation displays three very important characteristics:

- i. It results from a radical chain process. An important characteristic of such processes is that it is possible to envisage an inhibition, i.e. a polymer stabilization using, for instance, radical traps (antioxidants).
- ii. Radical chains are mainly initiated by hydroperoxide decomposition. This latter reaction is mainly characterized by a low activation energy (typically 80–140 kJ.mol⁻¹) linked to the low dissociation energy of the O–O bond (140–160 kJ.mol⁻¹). The activation energy of the thermolytic decomposition of polymers in the absence of oxygen is higher than 200 kJ.mol⁻¹. This is the reason why, when oxygen is present, oxidation always predominates over all the other reactions, at least in the temperature domain of practical interest, i.e. typically below 200°C in most cases.
- iii. Oxidation is kinetically controlled by the oxygen diffusion into the polymer. In other words, in bulk samples, oxidation is restricted to a superficial layer of thickness ℓ . As

it has been shown in the third section of this chapter, ℓ can be estimated using a scaling law. Moreover, the temperature effect on oxygen diffusivity D and on oxidation pseudo first rate constant K can be approximated by an Arrhenius law. It can be thus written (Audouin et al. 1994):

$$\ell = (D/K)^{1/2} = \left(\frac{D_0 \exp(-E_D/RT)}{K_0 \exp(-E_K/RT)} \right)^{1/2} = \ell_0 \exp\left(-\frac{E_\ell}{RT}\right) \quad (54)$$

where $\ell_0 = \left(\frac{D_0}{K_0} \right)^{1/2}$ and $E_\ell = \frac{1}{2}(E_D - E_K)$

Since, generally, $E_D < E_K$, the apparent activation energy of ℓ is negative, i.e. ℓ is a decreasing function of temperature, that induces two important consequences:

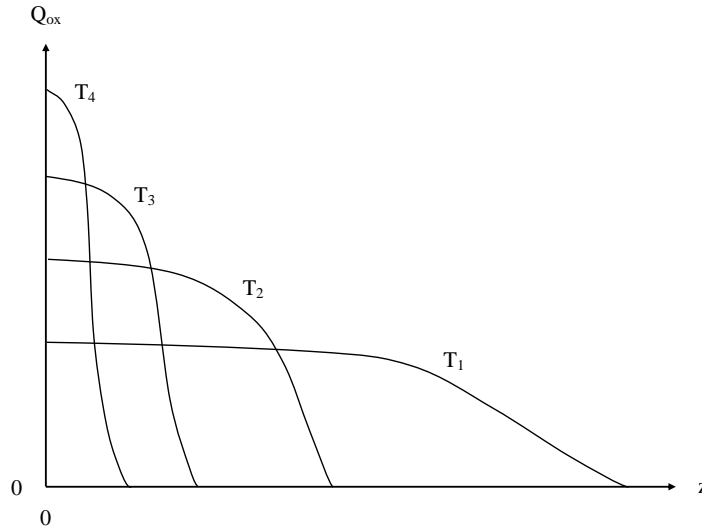


Figure 12. Schematic shape of oxidation profiles at four temperatures: $T_1 < T_2 < T_3 < T_4$.

First, the thickness of oxidation profiles is expected to vary with temperature as schematized in Figure 12.

Q_{ox} is the quantity of grafted oxygen. Z is the depth of the layer in the sample thickness.

It appears thus that if the chosen mode of accelerated ageing is simply to increase temperature, one can expect not only a quantitative change, i.e. an increase of oxidation rate, but also a qualitative change which can have important consequences on certain use properties, for instance mechanical ones.

Second, let us consider the thermolytic decomposition of polymer. It is, generally, a radical process inhibited by oxygen for the reason which can be schematized as follows:





The rate constant of oxygen addition to radicals (k_2) is extremely high (10^8 – 10^9 l.mol⁻¹.s⁻¹) and its activation energy is very low, close to zero. Thus, the reaction (Th) can compete with reaction (II) only at very high temperature and low oxygen concentration. Indeed, in the sample core where oxygen has no access, thermal decomposition can occur. This is the reason why thermal ageing tests made over a large temperature interval, for instance thermogravimetry, lead to an Arrhenius plot having the shape of Figure 13.

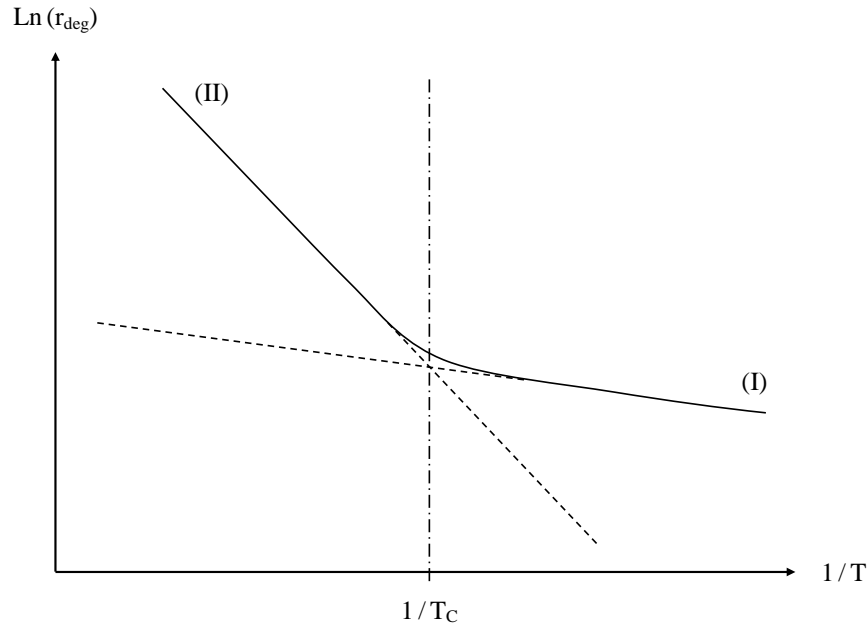


Figure 13. Shape of the Arrhenius plot of polymer degradation over a large temperature interval.

One can clearly distinguish two domains: (I) At low temperature, predominating oxidation; (II) At high temperature, predominating thermolytic decomposition.

This characteristic, as well as the one schematized in the previous Figure, shows that ultra-accelerated ageing tests at very high temperature are not pertinent when the objective is to predict the behaviour at service temperature, generally below the glass transition temperature of polymer. In this latter temperature domain, thermolytic decomposition is generally negligible, thermal ageing is mainly due to oxidation (eventually combined with post-cure).

2. Oxidation Mechanisms and Kinetics

The discovery of oxidation radical chain mechanism is often attributed to the English (RAPRA) group of Bolland (1946) although the true pioneer of the discipline is rather Semenov (Nobel Award 1956) (Semenov 1935). The first schemes start from the assumption

of an undefined radical source, producing radicals at a rate r_i in a medium where oxygen is in excess and hydroperoxides are stable. The mechanistic scheme is thus:



The kinetic scheme derived from the mechanism is composed of two equations:

$$\frac{d[\text{P}^\circ]}{dt} = r_i - k_2[\text{O}_2][\text{P}^\circ] + k_3[\text{PH}][\text{PO}_2^\circ] \quad (55)$$

$$\frac{d[\text{PO}_2^\circ]}{dt} = k_2[\text{O}_2][\text{P}^\circ] - k_3[\text{PH}][\text{PO}_2^\circ] - 2k_6[\text{PO}_2^\circ]^2 \quad (56)$$

Assuming steady-state for radical concentration:

$$\frac{d[\text{P}^\circ]}{dt} + \frac{d[\text{PO}_2^\circ]}{dt} = 0 \quad (57)$$

$$\begin{aligned}
 \Rightarrow r_i &= 2k_6[\text{PO}_2^\circ]^2 \\
 \Rightarrow [\text{PO}_2^\circ] &= \left(\frac{r_i}{2k_6} \right)^{1/2}
 \end{aligned} \quad (58)$$

Thus:

$$\frac{d[\text{O}_2]}{dt} = -k_2[\text{O}_2][\text{P}^\circ] = -\left(r_i + k_3[\text{PH}]\left(\frac{r_i}{2k_6} \right)^{1/2} \right) \quad (59)$$

The kinetic chain length Λ is the number of propagation events per initiation event:

$$\Lambda = \frac{k_3[\text{PH}]\left(\frac{r_i}{2k_6} \right)^{1/2}}{r_i} = \frac{k_3[\text{PH}]}{(2r_i k_6)^{1/2}} \quad (60)$$

It is often assumed that $\Lambda \gg 1$, so that:

$$\frac{d[\text{O}_2]}{dt} \approx -\frac{d[\text{POOH}]}{dt} = -k_3[\text{PH}]\left(\frac{r_i}{2k_6} \right)^{1/2} \quad (61)$$

This model was used for a long time to interpret thermal oxidation results, despite the fact that many key assumptions are not appropriate. The most important one is, no doubt, the assumption that hydroperoxides are stable. As a matter of fact, hydroperoxides are highly unstable and decompose into radicals in three main pathways:

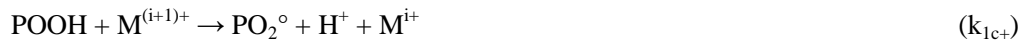
- Unimolecular decomposition:



- Bimolecular decomposition:



- Catalyzed decomposition:



- Balance reaction:



HO° and PO° radicals are several orders of magnitude more reactive than PO_2° ones. They abstract rapidly hydrogens to the polymer. PO° radicals can also rearrange into P° ones (see below). Thus, the above reactions can be rewritten:



In a first approach, these mechanisms will be not distinguished and it will be written:



Since hydroperoxides are especially unstable, they are expected to play a predominant role in initiation, so that the above mechanistic scheme becomes:



The corresponding kinetic scheme must be composed of three equations describing the concentration changes of P° , PO_2° and POOH :

$$\frac{d[P^\circ]}{dt} = \alpha k_1 [POOH]^\delta - k_2 [O_2][P^\circ] + k_3 [PH][PO_2^\circ] \quad (62)$$

$$\frac{d[PO_2^\circ]}{dt} = \beta k_1 [POOH]^\delta + k_2 [O_2][P^\circ] - k_3 [PH][PO_2^\circ] - 2k_6 [PO_2^\circ]^2 \quad (63)$$

$$\frac{d[POOH]}{dt} = -\delta k_1 [POOH]^\delta + k_3 [PH][PO_2^\circ] \quad (64)$$

There is a steady-state when the POOH formation by reaction (III) equilibrates their destruction by reaction (I). Then:

$$\frac{d[POOH]}{dt} = 0 \quad (65)$$

$$\Rightarrow [PO_2^\circ]_S = \frac{\delta k_1}{k_3 [PH]} [POOH]_S^\delta \quad (66)$$

where the subscript S indicates the steady-state.

Tobolsky and coll. (1950) used an ad hoc assumption to solve the problem: They assumed that there is a steady-state for radical concentration (Equ. 57), so that:

$$\begin{aligned} (\alpha + \beta) k_1 [POOH]^\delta &= 2k_6 [PO_2^\circ]^2 \\ \Rightarrow [PO_2^\circ]_S &= \left(\frac{\alpha + \beta}{2k_6} k_1 \right)^{1/2} [POOH]_S^{\delta/2} \end{aligned} \quad (67)$$

For the uncatalyzed oxidation, $\alpha + \beta = 2$ in both cases, so that:

$$[POOH]_S = \left(\frac{k_3 [PH]}{\delta (k_1 k_6)^{1/2}} \right)^{2/\delta} \quad (68)$$

$$\text{And } [PO_2^\circ]_S = \frac{k_3 [PH]}{\delta k_6} \quad (69)$$

The behavior during the transient depends on the molecularity (δ) of the POOH decomposition and the initial POOH concentration $[POOH]_0$. It is schematized in Figure 14.

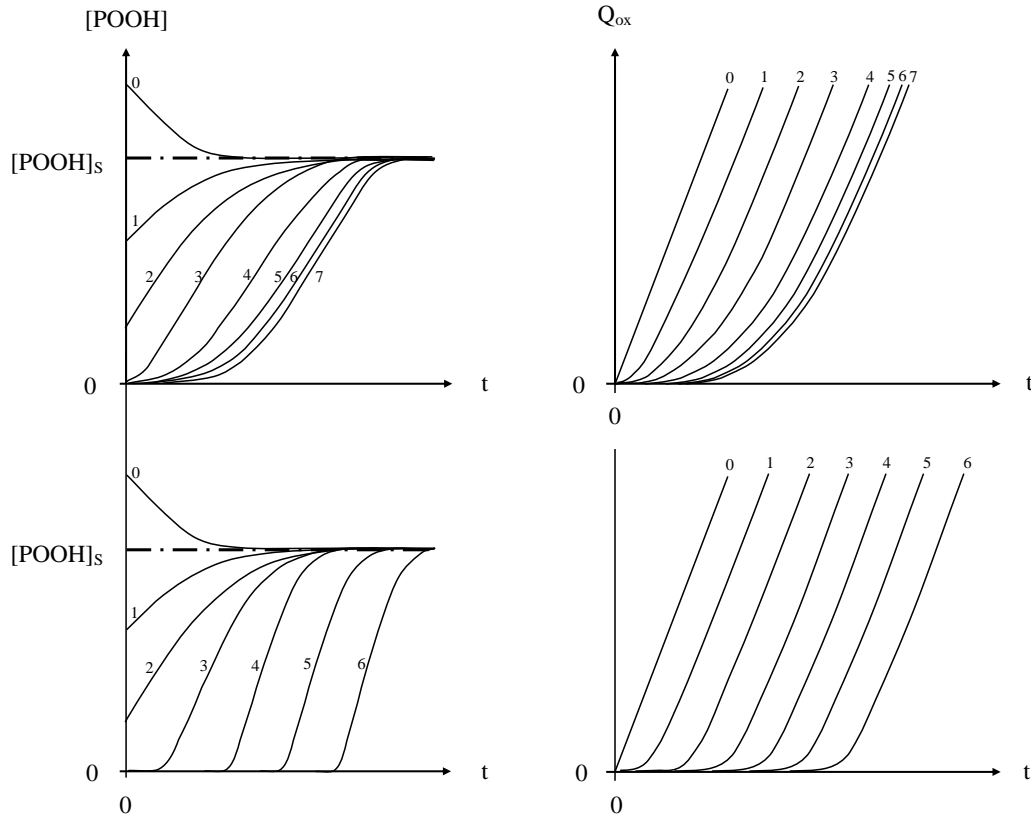


Figure 14. Shape of theoretical kinetic curves of hydroperoxide build-up (left) or stable oxidation products build-up (right) in the case of unimolecular (up) and bimolecular POOH decomposition (bottom), for various initial hydroperoxide concentrations $[\text{POOH}]_0$ decreasing from 0 to 7.

The kinetics display an induction period which can be defined as the time to reach the steady-state. Its characteristics differ with the mode of POOH decomposition (Audouin et al. 2000). In the case of unimolecular POOH decomposition, the conversion increases pseudo-exponentially. The induction time t_i is a decreasing function of the initial POOH concentration displaying an asymptote:

$$t_i \rightarrow \frac{3}{k_{1u}} \text{ when } [\text{POOH}]_0 \rightarrow 0 \quad (70)$$

In the case of bimolecular POOH decomposition, the conversion increases abruptly at the end of the induction period and the induction time increases logarithmically when the initial POOH concentration decreases. At low $[\text{POOH}]_0$ values:

$$t_i \rightarrow \frac{3}{k_3[\text{PH}](k_{1b}/2k_6)^{1/2}} \text{Ln} \frac{[\text{POOH}]_s}{[\text{POOH}]_0} \quad (71)$$

where $[\text{POOH}]_s$ is the steady-state POOH concentration.

In fact, indeed, both POOH decomposition modes coexist and the unimolecular mode becomes always predominant at low POOH concentration. This is the reason why the t_i variation with $[\text{POOH}]_0$ displays always the shape of Figure 15.

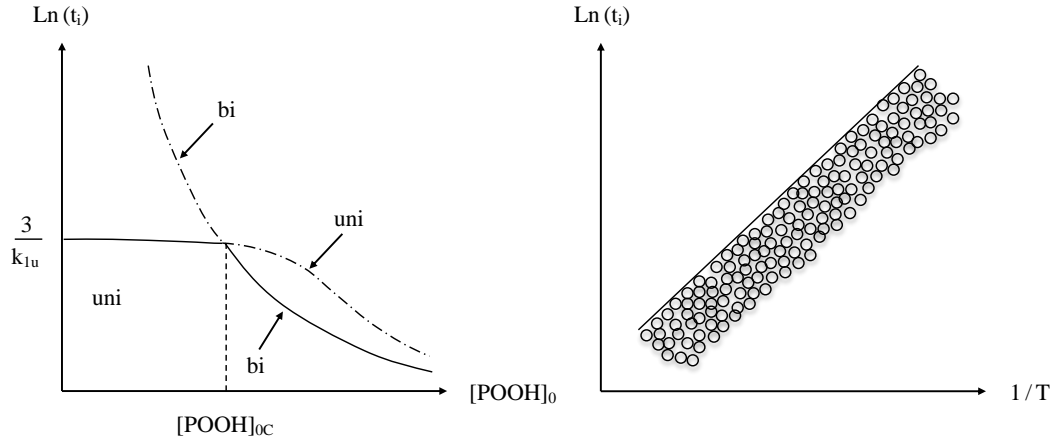


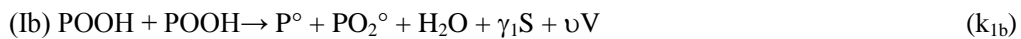
Figure 15. Effect of the initial POOH concentration on the induction period (left) in the case of pure unimolecular (uni) and pure bimolecular (bi) POOH decomposition. The full line represents the true dependence. Consequence of this dependence on the scatter of induction time values represented on an Arrhenius plot (right).

One can define a critical POOH concentration: $[\text{POOH}]_{0c}$ separating the unimolecular regime from the bimolecular one. Schematically, when $[\text{POOH}]_0 \leq [\text{POOH}]_{0c}$, the induction time is maximum and independent of $[\text{POOH}]_0$. When $[\text{POOH}]_0 > [\text{POOH}]_{0c}$, the induction time decreases logarithmically with $[\text{POOH}]_0$. This dependence explains the characteristic feature of Arrhenius plots of compiled t_i values coming from various sources (Richaud et al. 2008). The clouds of points display a relatively sharp upper boundary corresponding to the asymptotic value of t_i . They display also a relatively low scatter linked to the fact that, in bimolecular regime, t_i varies slowly with $[\text{POOH}]_0$.

It appears thus necessary to take into account both uni and bimolecular POOH decomposition processes in kinetic model, that imposes the use of numerical methods for their resolution.

3. KINETIC MODELING

The following mechanistic scheme is valid, at least in a first approach, in a wide variety of cases:





The following system of differential equations can be derived:

$$\frac{d[P^{\circ}]}{dt} = 2k_{1u}[POOH] + k_{1b}[POOH]^2 - k_2[O_2][P^{\circ}] + k_3[PH][PO_2^{\circ}] - 2k_4[P^{\circ}]^2 \quad (72)$$

$$-k_5[P^{\circ}][PO_2^{\circ}]$$

$$\frac{d[PO_2^{\circ}]}{dt} = k_{1b}[POOH]^2 + k_2[O_2][P^{\circ}] - k_3[PH][PO_2^{\circ}] - k_5[P^{\circ}][PO_2^{\circ}] - 2k_6[PO_2^{\circ}]^2 \quad (73)$$

$$\frac{d[POOH]}{dt} = -k_{1u}[POOH] - 2k_{1b}[POOH]^2 + k_3[PH][PO_2^{\circ}] \quad (74)$$

$$\frac{d[PH]}{dt} = -\mu_{1u}k_{1u}[POOH] - \mu_{1b}k_{1b}[POOH]^2 + k_3[PH][PO_2^{\circ}] \quad (75)$$

$$\frac{d[O_2]}{dt} = D \frac{\partial^2 [O_2]}{\partial z^2} - k_2[O_2][P^{\circ}] + k_6[PO_2^{\circ}]^2 \quad (76)$$

$$\frac{dS}{dt} = \gamma_1 k_{1u}[POOH] + \gamma_1 k_{1b}[POOH]^2 \quad (77)$$

$$\frac{dX}{dt} = \gamma_4 k_4 [P^{\circ}]^2 \quad (78)$$

γ_1 and γ_4 , μ_1 and μ_2 are dimensionless yield values, generally lower than unity.

V is the “average volatile molecule” of which the molar mass M_V corresponds to the number average molar masses of true volatile molecules. υ is the number average yield of volatile molecules.

The boundary conditions are:

At $t = 0$, for all the sample thickness: $[P^{\circ}] = 0$, $[PO_2^{\circ}] = 0$, $[POOH] = [POOH]_0$ and $[O_2] = [O_2]_S$ (equilibrium oxygen concentration for the oxygen partial pressure under consideration).

At $t > 0$: $[O_2] = [O_2]_S$ at superficial layers: $z = 0$ and $z = L$.

These equations allow to determine the weight variation. In an elementary layer, it can be written (Colin et al. 2002):

$$\left(\frac{dm}{dt}\right)_z = \frac{32}{\rho} \frac{d[O_2]}{dt} - \frac{18}{\rho} \frac{d[H_2O]}{dt} - \frac{\nu M_V}{\rho} \frac{d[V]}{dt} \quad (79)$$

So that:

$$\left(\frac{dm}{dt}\right)_z = \frac{32}{\rho} k_2 [O_2]_z [P^\bullet]_z - \left[\frac{32}{\rho} k_6 [PO_2^\bullet]_z^2 + \left(\frac{18}{\rho} + \frac{\nu M_V}{\rho} \right) (k_{1u} [POOH]_z + k_{1b} [POOH]_z^2) \right] \quad (80)$$

It is noteworthy that mass gain (linked to oxygen reaction with radicals) occurs only in propagation processes, whereas mass loss occurs exclusively in initiation or termination processes. It results that the balance weight loss / weight gain must be sharply linked to the kinetic chain length Λ . An interesting property of the mechanistic scheme under consideration is that Λ decreases continuously during the induction time to reach a value close to unity in steady state. One can generally expect three main kinds of gravimetric behaviors (in isothermal conditions) as schematized in Figure 16.

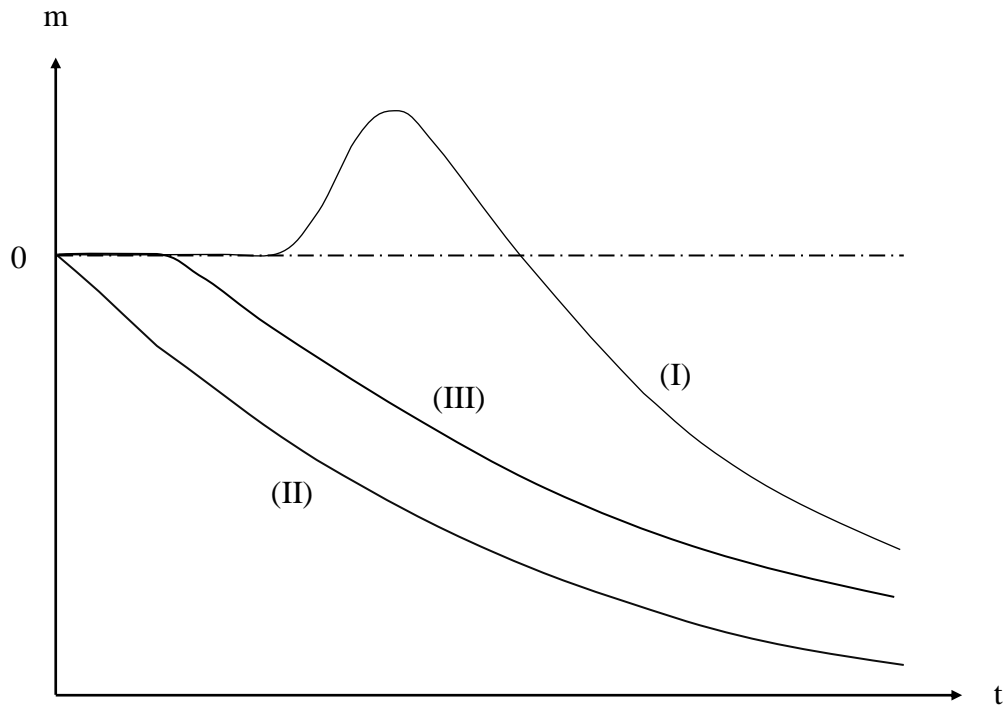


Figure 16. Shape of isothermal gravimetric curves for polymer oxidation (see text).

When the induction period phenomenon is well marked, the initial kinetic chain length is high, mass gain predominates over mass loss in the early period of exposure. When the end of the induction period approaches, the kinetic length decreases at a point where mass loss becomes predominant. In steady-state, the mass loss rate is constant. At long term, however,

the whole oxidation rate decreases as a consequence of substrate consumption, and the mass loss rate decreases (regime I).

In the absence of significant induction period, the initial kinetic chain length is low and mass loss predominates as soon as exposure begins (regime II).

Indeed, an intermediary behaviour (regime III) can be observed. It is noteworthy that a given polymer can degrade in regime (I) at low temperature and in regime (II) at high temperature. In regime (I), the amplitude of mass gain depends on the size and yield of volatile molecules.

The ability of the above kinetic model to simulate gravimetric curves having a wide variety of shapes, including non monotonous ones, can be considered as a strong argument in favour of the model validity, especially if it predicts at the same time oxidation thickness profiles.

4. Spontaneous Cracking Induced by Oxidation

Oxidation in a superficial layer induces a weight change, as seen above, and, at least in polymers based predominantly on C and H atoms, a density (ρ) increase due to the fact that oxygen atom is heavier than C or H atoms (Pascault et al. 2002). There is thus a volume change of the oxidized layer:

$$\frac{\Delta v}{v} = \frac{\Delta m}{m} - \frac{\Delta \rho}{\rho} \quad (81)$$

Since $\Delta \rho / \rho$ is generally positive, it can be seen that the oxidized layer tends to shrink if $\Delta m / m$ is negative, i.e. when weight loss predominates over weight gain. Since shrinkage is hindered by the adhesion of the oxidized layer to the sample core, a stress state is induced. At the same time, the oxidized layer undergoes embrittlement (section 2). One can thus schematize the sample behaviour as follows: The local stress σ in the oxidized layer increases with the exposure time, whereas the ultimate stress σ_u decreases as a result of polymer degradation. Cracking must occur when σ becomes equal to σ_u . Gravimetric behaviours (I) and (II) are expected to induce two distinct cracking behaviours (Figure 17).

In the case of gravimetric behaviour of type I, stresses develop only at the end of the induction period, when mass loss begins. Cracks can thus initiate only after the end of induction period. But chain scission occurs during the induction period, so that the oxidized layer can be noticeably embrittled when cracks initiate. As a result, cracks are expected to propagate rapidly through the oxidized layer. In the case of gravimetric behaviour of type II, stresses develop as soon as exposure begins. One can thus imagine cases where cracking begins at a moment where the toughness of the oxidized layer remains relatively high. Then, cracks are expected to propagate comparatively slowly, at a rate mainly determined by the local changes of polymer toughness. Amine crosslinked epoxies are typical of this last behaviour, whereas poly(bismaleimide) are typical of the former one (Colin et al. 2005). In composites, indeed, matrix shrinkage is expected to induce also fiber debonding (Lafarie-Frenot et al. 2010).

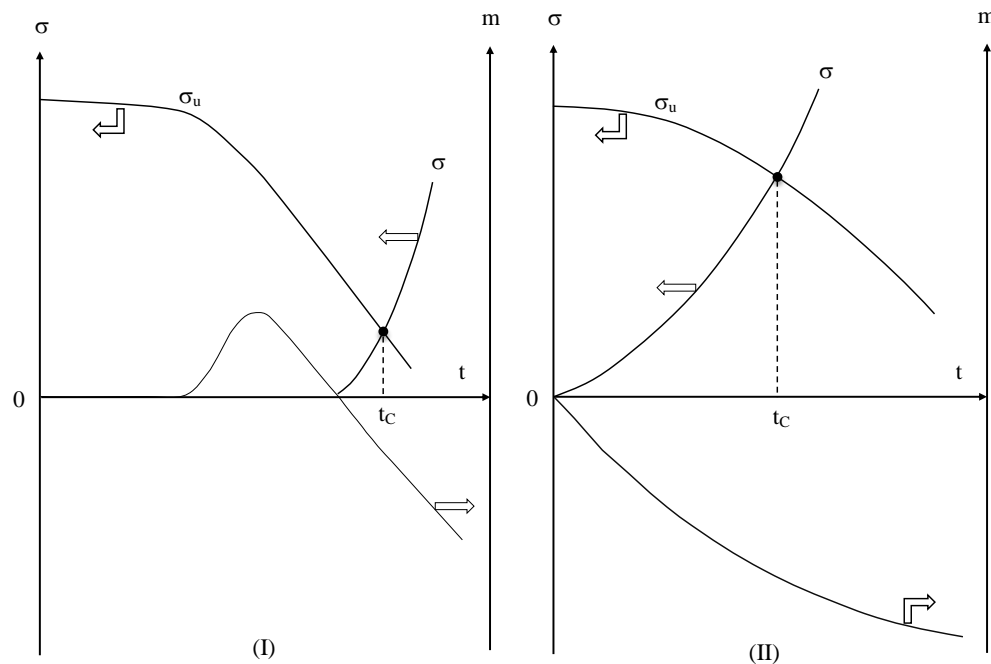


Figure 17. Spontaneous cracking conditions in the case of gravimetric behaviour of type (I) (left) and (II) (right).

CONCLUSIONS

The main modes of physico-chemical ageing for organic matrix composites are hydrolysis (especially important for the most common class of resin composites, i.e. glass fibers/unsaturated polyesters) and thermal oxidation (responsible for superficial cracking and embrittlement in many parts of aeronautic engines or structural parts of supersonic aircrafts). Both hydrolysis and oxidation processes have in common to induce chain scission, this latter being responsible for embrittlement at low conversions. The quantitative relationships between macromolecular structure and number of chain scissions on one side, and between macromolecular structure and fracture properties on the other side, are recalled. Embrittlement mechanisms are relatively well elucidated in the case of linear polymers, but remain an open problem in thermosets.

Hydrolysis and oxidation have also in common to have their kinetics eventually controlled by the diffusion of a small molecule (water or oxygen) coming from environment. This control leads to the confinement of degradation processes in more or less thick superficial sample layers, that carries important consequences on use properties. The characteristics of oxidized layers can be predicted from equations coupling diffusion and reaction rate processes. These equations are relatively simple in the case of hydrolysis, but can be highly complex in the case of oxidation where they need several simplifying assumptions to be analytically solved.

Hydrolysis mechanisms and kinetics were established long time ago. Complications in kinetic modelling can appear in the presence of catalytic processes, especially because the

solubility of catalytic species (ions) in polymer matrices is difficult to determine. In the case of unsaturated polyesters, osmotic cracking induced by hydrolysis is a very important process, responsible for blistering of boats, swimming pools, etc ... Its mechanism is now relatively well understood. Oxidation mechanisms were established one half century ago, but kinetic modelling remained a challenging objective for a long time, especially when reaction–diffusion coupling is needed.

The recent introduction of numerical methods allowed to suppress many oversimplifying assumptions and opens now the way to efficient lifetime predictions. The first decade of 21st century will probably appear, in the future, as the transition period between the empirical area of polymer ageing and the modern area where lifetime prediction will be a fully scientific approach.

REFERENCES

- Abeysinghe H.J., Ghotra J.S., Pritchard G., Substances contributing to the generation of osmotic pressure in resins and laminates, *Composites* 14, 57-61 (1983).
- Ashbee K.H.G., Wyatt R.C., Water damage in glass fibre/resin composites, *Proceedings of the Royal Society A* 312, 553-564 (1969).
- Audouin L., V. Langlois, J. Verdu and J.C.M. De Bruijn, Role of oxygen diffusion in polymer ageing: kinetic and mechanical aspects, *Journal of Materials Science* 29(3), 569-583 (1994).
- Audouin L., Achimsky L., Verdu J., “Modelling of Hydrocarbon Polymer Oxidation“, in *Handbook of Polymer Degradation*, 2nd edition, S. Halim Hamid ed., Marcel Dekker, New-York, Chap. 20, pp. 727-763, 2000.
- Ballara A., Verdu J., Physical aspects of the hydrolysis of polyethylene terephthalate, *Polymer Degradation and Stability* 26, 361-374 (1989).
- Belan F., Bellenger V., Mortaigne B., Verdu J., Relationship between the structure and hydrolysis rate of unsaturated polyester prepolymers, *Polymer Degradation and Stability* 56, 301-309 (1997).
- Bellenger V., Verdu J., Ganem M., Mortaigne B., Styrene crosslinked vinylesters. II: Water sorption, water diffusion and cohesive properties, *Polymer and Polymer Composites* 2(1), 17-25 (1994).
- Bellenger V., Ganem M., Mortaigne B., Verdu J., Lifetime prediction in the hydrolytic ageing of polyesters, *Polymer Degradation and Stability* 49(1), 91-97 (1995).
- Bicerano J., *Prediction of Polymer Properties*, 3rd edition, Marcel Dekker, New-York, 2002.
- Bolland J.L., Kinetic studies in the chemistry of rubber and related materials. I. The thermal oxidation of ethyl linoleate, *Proceedings of the Royal Society A* 186, 218-236 (1946).
- Carter H.G., Kibler K.G., Lagmuir-type model for anomalous moisture diffusion in composite resins, *Journal of Composite Materials* 12, 118-131 (1978).
- Charlesby A., Pinner S.H., Analysis of the solubility. Behaviour of irradiated polyethylene and other polymers, *Proceedings of the Royal Society A* 249, 367-386 (1959).
- Colin X., Marais C., Verdu J., Kinetic modeling and simulation of gravimetric curves: application to the oxidation of bismaleimide and epoxy resins, *Polymer Degradation and Stability* 78(3), 545-553 (2002).

- Colin X., Mavel A., Marais C., Verdu J., Interaction between cracking and oxidation in organic matrix composites, *Journal of Composite Materials* 39(15), 1371-1389 (2005).
- Coquillat M., Verdu J., Colin X., Audouin L., Nevière R., Thermal oxidation of polybutadiene, *Polymer Degradation and Stability* 92(7), 1326-1333, 1334-1342 and 1343-1349 (2007).
- Coquillat M., Audouin L., Verdu J., to be published in 2010.
- Cunliffe A.V., Davis A., Photo-oxidation of thick polymer samples. Part II: The influence of oxygen diffusion on the natural and artificial weathering of polyolefins, *Polymer Degradation and Stability* 4(1), 17-37 (1982).
- Crank J., Park G.S., *Diffusion in polymers*, Academic Press, London, 1968.
- Crawford C.D., Lesser A.J., Brittle to ductile fracture toughness mapping on controlled epoxy networks, *Polymer Engineering and Science* 39(2), 385-392 (1999).
- Derrien K., Gilormini P., Interaction Between Stress and Diffusion in Polymers, in *Proceedings of the DSL 2006 Conference, Defect and Diffusion Forum* 258/260, pp. 447-452, 2006.
- Di Benedetto A.T., Scola D.A., Characterization of S-glass/polysulfone adhesive failure using ion scattering spectroscopy and secondary ion mass spectrometry, *Journal of Colloid and Interface Science* 74(1), 150-162 (1980).
- Di Benedetto A.T., Lex P.J., Evaluation of surface treatments for glass fibers in composite materials, *Polymer Engineering and Science* 29(8), 543-555 (1989).
- Di Marzio E.A., On the second-order transition of rubber, *Journal of Research of the National Bureau of Standards: Section A: Physics and Chemistry* 68, 611-617 (1964).
- Fayolle B., Audouin L., Verdu J., Initial steps and embrittlement in the thermal oxidation of stabilized polypropylene films, *Polymer Degradation and Stability* 75(1), 123-129 (2002).
- Fayolle B., E. Richaud, X. Colin and J. Verdu, Review: Degradation-induced embrittlement in semi-crystalline polymers having their amorphous phase in rubbery state, *Journal of Materials Science* 43, p. 6999-7012 (2008).
- Fayolle B., Verdu J., Piccoz D., Dahoun A., Hiver J.-M., G'Sell C., Thermooxidative ageing of polyoxymethylene. Part 2: Embrittlement mechanisms, *Journal of Applied Polymer Science* 111, 469-475 (2009).
- Fedors R.F., Osmotic effects in water absorption by polymers, *Polymer* 21, 207-212 (1980).
- Fetters L.J., Lohse D.J., Graessley W.W., Chain dimensions and entanglement spacings in dense macromolecular systems, *Journal Polymer Science: Part B: Polymer Physics* 37, 1023-1033 (1999).
- Fox T.G., Flory P.J., The glass temperature and related properties of polystyrene. Influence of molecular weight, *Journal of Polymer Science* 14(75), 315-319 (1954).
- Flory P.J., *Principles of Polymer Chemistry*, Cornell University Press, Ithaca, New York, 1953.
- Ganem M., Mortaigne B., Bellenger V., Verdu J., Hydrolytic ageing of vinylester materials. Part 1: Ageing of prepolymers and model compounds, *Polymer Networks and Blends* 4(2), 87-92 (1994).
- Gaudichet-Maurin E., Thominet F., Verdu J., Water sorption characteristics in moderately hydrophilic polymers. Part 1: Effect of polar groups concentration and temperature in water sorption in aromatic polysulphones, *Journal of Applied Polymer Science* 109(5), 3279-3285 (2008).

- Gautier L., Mortaigne B., Bellenger V., Verdu J., Osmotic cracking nucleation in hydrothermal-aged polyester matrix, *Polymer* 41(7), 2481-2490 (1999).
- Greco R., Ragosta G., Influence of molecular weight on fracture toughness and fractography of glassy polymers, *Plastics and Rubber Processing and Applications* 7(3), 163-171 (1987).
- Hoh K.-P., Ishida H., Koenig J.L., Multi-nuclear NMR spectroscopic and proton NMR imaging studies on the effect of water on the silane coupling agent/matrix resin interface in glass fiber-reinforced composites, *Polymer Composites* 11(3), 192-199 (1990).
- Hopfenberg H.B., *Permeability of plastic films and coatings in gases, vapours and liquids*, Plenum Press, New York, 1978.
- Ishida H., Koenig J.L., A Fourier-transform infrared spectroscopic study of the hydrolytic stability of silane coupling agents on E-glass fibers, *Journal of Polymer Science: Part B: Polymer Physics* 18, 1931-1943 (1980).
- Ishida H., A review of recent progress in the studies of molecular and microstructure of coupling agents and their functions in composites, coatings and adhesive joints, *Polymer Composites* 5(2), 101-123 (1984).
- Jacques B., Werth M., Merdas I., ThomINETTE F., Verdu J., Hydrolytic ageing of polyamide 11. I. Hydrolysis kinetics in water, *Polymer* 43(24), 6439-6447 (2002).
- Kaelble D.H., Dynes P.J., Crane L.N., Maus L., Interfacial mechanisms of moisture degradation in graphite-epoxy composites, *The Journal Adhesion* 7(1), 25-54 (1975).
- Kaelble D.H., Dynes P.J., Maus L., Hygrothermal ageing of composite materials. Part 1: Interfacial aspects, *The Journal Adhesion* 8(2), 121-144 (1976).
- Kausch H.H., Heymans N., Plummer C.F., Decroly P., *Matériaux Polymères. Propriétés Mécaniques et Physiques*, Presses Polytechniques et Universitaires Romandes, Lausanne, Switzerland, 2001.
- Kennedy M.A., A.J. Peacock and L. Mandelkern, Tensile properties of crystalline polymers: linear polyethylene, *Macromolecules* 27(19), 5297-5310 (1994).
- Kondo K., Taki T., Moisture diffusivity of unidirectional composites, *Journal of Composite Materials* 16(2), 82-93 (1982).
- Lafarie-Frenot.M.C, Grandidier.J.C, Gigliotti.M, Olivier.L, Colin.X, Verdu.J and Cinquin.J. *Polym. Degrad. Stab.* (2010), 95, 965.
- Le Huy H.M., Bellenger V., Verdu J., Paris M., Thermal oxidation of anhydride cured epoxies. III. Effect on mechanical properties, *Polymer Degradation and Stability* 41(2) 149-156 (1993).
- McCall D.W., Douglass D.C., Blyler Jr. L.L., Johnson G.E, Jelinski L.W., Bair H.E., Solubility and diffusion of water in low-density polyethylene, *Macromolecules* 17(9), 1644-1649 (1984).
- McMahon W., Birdsall H.A., Johnson G.A., Camilli C.J., Degradation studies of polyethylene terephthalate, *Journal of Chemical and Engineering Data* 4, 57-79 (1959).
- Merdas I., ThomINETTE F., Tcharkhtchi A., Verdu J., Factors governing water absorption by composite matrices, *Composites Science and Technology* 62, 487-492 (2002).
- Merdas I., ThomINETTE F., Verdu J., Hydrolytic ageing of polyamide 11. Effect of carbon dioxide on polyamide 11 hydrolysis, *Polymer Degradation and Stability* 79, 419-425 (2003).
- Meyer A., Jones W., Lin Y. Kranbuehl D., Characterizing and modelling the hydrolysis of polyamide 11 in a pH 7 water environment, *Macromolecules* 35, 2784-2798 (2002).

- Mortaigne B., Bellenger V., Verdu J., Hydrolysis of styrene crosslinked unsaturated polyesters. Effect of chain ends, *Polymer Networks and Blends* 2, 187-195 (1992).
- Olivier L., C. Baudet, D. Bertheau, J.-C. Grandidier and M.-C. Lafarie-Frenot. Development of experimental, theoretical and numerical tools for studying thermo-oxidation of CFRP composites. *Composites: Part A: Applied Science and Manufacturing* 40, 1008-1016 (2009).
- Pascault J.-P., Sautereau H., Verdu J., Williams R.J.J., *Thermosetting Polymers*, Marcel Dekker, New-York, Chap. 10, pp. 282-321 and Chap. 14, pp. 420-467, 2002.
- Pitkethly M.J., Favre J.-P., Gaur U., Jakubowski J., Mudrich S.F., Caldwell D.L., Drzal L.T., Nardin M., Wagner H.D., Di Landro L., Hampe A., Armistead J.P., Desaegeer M., Verposet I., *Composites Science and Technology* 48, 205-214 (1993).
- Pryde C.A., Kelleher P.G., Hellman M.Y., Wentz R.P., The hydrolytic stability of some commercially available polycarbonates, *Polymer Engineering and Science* 22(6), 370-375 (1982).
- Rasoldier N., Colin X., Verdu J., Bocquet M., Olivier L., Chocinski-Arnault L., Lafarie-Frenot M.-C., *Composites: Part A: Applied Science and Manufacturing* 39, 1522-1529 (2008).
- Ravens D.A.S., The Chemical reactivity of poly(ethylene terephthalate). Heterogeneous hydrolysis by hydrochloric acid, *Polymer* 1, 375-383 (1960).
- Richaud E., Colin X., Fayolle B., Verdu J., Induction period in the low temperature thermal oxidation of saturated hydrocarbons: Example of polyethylene, *International Journal of Chemical Kinetics* 40(12), 769-777 (2008).
- Richaud E., Ferreira P., Audouin L., Colin X., Verdu J., Monchy-Leroy C., Radiochemical ageing of poly(ether ether ketone), *European Polymer Journal* 46, 731-743 (2010).
- Rosen M.R., Goddard E.D., FDT: a technique for direct study of water attack at the silane-fiber interface, *Polymer Engineering and Science* 20, 413-425 (1980).
- Roy S., Singh S., Analytical modelling of orthotropic diffusivities in a fiber reinforced composite with discontinuities using homogenization, *Composites Science and Technology*, in press (2010).
- Saito O., On the effects of high energy radiation to polymers. I. Crosslinking and degradation, *Journal of the Physical Society of Japan* 13(2), 198-206 (1958a).
- Saito O., On the effects of high energy radiation to polymers. II. End-linking and gel fraction, *Journal of the Physical Society of Japan* 13(12), 1451-1464 (1958b).
- Salmon L., ThomINETTE F., Pays M.-F., Verdu J., Hydrolytic aging of polysiloxane networks modelling the glass fiber epoxy-amine interphase, *Composites Science and Technology* 57, 1119-1127 (1997).
- Sargent J.P., Ashbee K.H.G., Very slow crack growth during osmosis in epoxy and in polyester resins, *Journal of Applied Polymer Science* 29(3), 809-822 (1984).
- Schrader M.E., Block A., Tracer study of kinetics and mechanism of hydrolytically induced interfacial failure, *Journal of Polymer Science: Part C: Polymer Letters* 34, 281-291 (1971).
- Schutte L.L., Mc Donough W., Shioya M., Mcauliffe M., Greenwood M., The use of a single-fibre fragmentation test to study environmental durability of interfaces/interphases between DGEBA/mPDA epoxy and glass fibre: the effect of moisture, *Composites* 25(7), 617-624 (1994).

- Seguchi T., Arakawa K., Hayakawa W., Watanabe Y., Kuryama I., Radiation induced oxidative degradation of polymers. I. Oxidation region in polymer films irradiated in oxygen under pressure, *Radiation Physics and Chemistry* 17(4), 195-201 (1981).
- Seguchi T., Arakawa K., Hayakawa W., Watanabe Y., Kuryama I., Radiation induced oxidative degradation of polymers. II. Effects of radiation on swelling and gel fraction of polymers, *Radiation Physics and Chemistry* 19(4), 321-327 (1982).
- Semenov N.N., *Chemical kinetics and chain reactions*, Oxford University Press, London, 1935.
- Serpe G., Chaupart N., Verdu J., Ageing of polyamide 11 in acid solutions, *Polymer* 38(8), 1911-1917 (1997).
- Shen C.H., Springer G.S., Moisture absorption and desorption of composite materials, *Journal of Composite Materials* 10(1), 2-20 (1976).
- Tcharkhtchi A., Bronnec Y., Verdu J., *Polymer* 41(15), Water absorption characteristics of diglycidylether of butane diol-3,5-2,4-diaminotoluene networks, 5777-5785 (2000).
- Thomason J.L., Investigation of composite interphase using dynamic mechanical analysis: artifacts and reality, *Polymer Composites* 11(2), 105-113 (1990).
- Thominette F., Gaudichet-Maurin E., Verdu J., Effect of structure on water diffusion in moderately hydrophilic polymers, in *Proceedings of the DSL 2006 Conference, Defect and Diffusion Forum* 258/260, pp. 442-446, 2006.
- Tobolsky A.V., Metz D.J., Mesrobian R.B., Low temperature autoxidation of hydrocarbons: the phenomenon of maximum rates, *Journal of American Chemical Society* 72(2), 1942-1952 (1950).
- Van Krevelen D.W. and Hoftyzer P.J., *Properties of Polymers. Their Estimation and Correlation with Chemical Structure*, 3rd edition, Elsevier, Amsterdam, Chap. 18, pp. 412-413, 1976.
- Van't Hoff J., The function of osmotic pressure in the analogy between solutions and gases, *Philosophical Magazine* 26(5), 81-105 (1888).
- Walter E., Ashbee K.H.G., Osmosis in composites materials, *Composites* 13(4), 365-368 (1982).